Physics – Uspekhi **47** (11) 1075 – 1099 (2004)

REVIEWS OF TOPICAL PROBLEMS PACS numbers: 61.50.Ah, 63.20.Dj, 71.15.Mb

Ab initio calculations of the physical properties of ionic crystals

E G Maksimov, V I Zinenko, N G Zamkova

DOI: 10.1070/PU2004v047n11ABEH001796

Contents

Abstract. First-principles calculations of the physical properties of ionic crystals are reviewed. Two markedly different approaches within the framework of the density functional theory are described. In one of them, the electron spectrum and wave functions are treated within the standard band picture based on the solution of Kohn – Sham equations. In the second approach, the total electron density of a crystal is represented as a superposition of the densities of individual ions. The problem of determining the electric polarization of a crystal is discussed for each approach. It is shown that it is the use of Bloch functions rather than the physics of the phenomenon that complicates the solution of this problem within the Kohn – Sham framework. The deformable and polarizable ion model is described in detail, and its application to calculating many properties of ionic crystals, including the lattice dynamics and structural stability of crystal phases, is discussed.

1. Introduction

We begin with definitions. *Ab initio* (first-principles) calculations of physical properties of crystals are calculations that use no adjustable parameters and phenomenological models. The only information in such calculations is the atomic number in the Periodic Table, i.e., the knowledge about the number of electrons in a given atom and its atomic weight. The calculation is based on the use of the laws of quantum mechanics and statistical physics. Interestingly, ionic crystals, precisely alkali-halide compounds, were the first objects of such calculations in the early 1930s [1]. These calculations used an approximate quantum-mechanical theory of many-body systems, proposed by Thomas [2] and Fermi [3]. Jensen and Lenz [1] were able to calculate, with fairly high accuracy, the equilibrium volumes, elastic constants, and bulk moduli of several alkali-halide crystals.

However, the Thomas – Fermi theory, while formally being an exact theory at ultrahigh pressures, at normal pressures describes the properties of crystals with moderate accuracy [4]. To increase the accuracy, one must at least take into account that the system's energy depends not only on the electron density but also on the gradients of this density [5]. In their review, Kirzhnits et al. [6] presented a generalized version of the Thomas – Fermi theory.

For a long time after the initial work of Jensen and Lenz [1] no attempts were made to carry out first-principles calculations of ionic crystals, and phenomenological models were used in the theory of such crystals [7 – 10]. All these models are based on the idea of an ionic crystal as a system consisting of individual ions whose electron densities (or wave functions) may overlap. These ions interact with each other through long-range Coulomb attraction and short-range repulsion due to the overlap of their electron shells. An external field could polarize the ions, which acquire a dipole moment. Such perturbation can be produced either by an external electric field or by shifts of the ions in the crystal, e.g., in the vibration of an optically active phonon mode. The value of the respective dipole moment is also determined by the ion deformation caused by short-range interaction with the nearest surroundings. The total electron polarization of the crystal is defined in this case as the sum of the dipole moments of individual ions. Within the framework of these phenomenological models methods for calculating various physical properties of crystals, including the phonon spectra of crystals, were developed.

It must be noted that beginning with the classical works of Löwdin [11] and Tolpygo [12], attempts were made to justify the phenomenological models of ionic crystals, which allowed for polarizability and deformations of ions. This approach was based on the quantum-mechanical treatment of ionic crystals, which allowed for the overlap of the wave functions

E G Maksimov P N Lebedev Physics Institute,
Russian Academy of Sciences,
Leninskiĭ prosp. 53, 119991 Moscow, Russian Federation
Tel. (7-095) 135 75 11. Fax (7-095) 135 85 33
E-mail: maksimov@lpi.ru
V I Zinenko, N G Zamkova L V Kirenskiĭ Institute of Physics,
Siberian Division of the Russian Academy of Sciences,
Akademgorodok, 660036 Krasnoyarsk, Russian Federation
Tel. (7-3912) 43 29 06. Fax (7-3912) 43 89 23
E-mail: zvi@iph.krasn.ru

Received 8 January 2004
Uspekhi Fizicheskikh Nauk **174** (11) 1145 – 1170 (2004)
Translated by E Yankovsky; edited by M V Magnitskaya

of individual ions. Here, the total energy of a crystal was determined by the Coulomb interaction of ions and various overlap integrals of the wave functions. Similar attempts of calculating the physical properties of ionic crystals were repeated [13, 14]. Unfortunately, real calculations have been done only for the simplest ionic crystals of the LiH type. For more complicated compounds insurmountable difficulties arise within this approach, difficulties related to the huge volume of calculations involving the numerous overlap integrals and the very wave functions of the ions.

As for the lattice dynamics of ionic crystals, a (formally) exact formulation of such dynamics has existed for thirty years [15]. This approach uses an expression for the electron contribution to the dynamical matrix in terms of the dielectric matrix $\varepsilon(\mathbf{q}+\mathbf{K},\mathbf{q}+\mathbf{K}')$ in the space of the reciprocal lattice vectors $\mathbf{K}$ and $\mathbf{K}'$. It can be demonstrated (see the review article in Ref. [16]) that the expression for the dynamical matrix can be formally reduced to the same form as in the classical phenomenological models of lattice vibrations. Unfortunately, it has proven very difficult to really calculate the vibration frequencies, the dielectric constant, and the effective dynamical charges.

Actually, first-principles calculations of physical properties of crystals, including ionic crystals, began with the development of density functional theory, formulated in the works of Kohn, Hohenberg, and Sham [17, 18]. The main ideas of this approach were expounded in Kohn's Nobel lecture [19].

2. The density functional theory

In 1964, Hohenberg and Kohn [17] formulated the fundamentals of the density functional theory. They showed that the ground-state energy of a system of interacting particles is a single-valued functional of the particle density distribution $\rho(\mathbf{r})$ and, hence, $\rho(\mathbf{r})$ implicitly determines all the properties of the ground state of a system of interacting particles. The true density distribution is given by the minimum of the energy functional

$$\frac{\delta E_{\rm el}\{\rho(\mathbf{r})\}}{\delta\rho(\mathbf{r})}=0\,. \tag{2.1}$$

We write the total energy of the electrons in a crystal in the form

$$E_{\rm el}\{\rho(\mathbf{r})\}=\int\rho(\mathbf{r})\varepsilon_{\rm k}\{\rho(\mathbf{r})\}\,{\rm d}\mathbf{r}+\int V_{\rm ext}(\mathbf{r})\,\rho(\mathbf{r})\,{\rm d}\mathbf{r} +\frac{e^2}{2}\iint\frac{\rho(\mathbf{r})\,\rho(\mathbf{r}')}{|\mathbf{r}-\mathbf{r}'|}\,{\rm d}\mathbf{r}\,{\rm d}\mathbf{r}'+\int\rho(\mathbf{r})\,\varepsilon_{\rm xc}\{\rho(\mathbf{r})\}\,{\rm d}\mathbf{r}\,. \tag{2.2}$$

Here, the first term is the kinetic energy of the electrons. The second term is the energy of interaction with an external field, which in the case of a crystal has the form

$$V_{\rm ext}(\mathbf{r})=\sum_n\frac{Z_n e^2}{|\mathbf{R}_n-\mathbf{r}|}\,, \tag{2.3}$$

where Z_n is the charge of the nucleus. The third term is the classical electron–electron interaction. Finally, the fourth term is the energy of the exchange-correlation interaction of electrons.

Of course, we do not know the exact expressions for the functionals of the kinetic and exchange-correlation energies. If we assume, however, that $\varepsilon_{\rm k}\{\rho(\mathbf{r})\}$ and $\varepsilon_{\rm xc}\{\rho(\mathbf{r})\}$ are local functionals of the density (i.e., depend only on the density $\rho(\mathbf{r})$ at a given point in space) and are determined by the form of the dependence on density for a homogeneous electron gas, we immediately get [4, 6, 19]

$$\begin{aligned}\varepsilon_{\rm k}\{\rho(\mathbf{r})\}&=\alpha\rho^{2/3}(\mathbf{r})\,,\\ \varepsilon_{\rm xc}\{\rho(\mathbf{r})\}&=\beta\rho^{1/3}(\mathbf{r})\,,\end{aligned} \tag{2.4}$$

where α and β are well-known numerical constants. Now, plugging (2.2)–(2.4) into (2.1) and varying the energy with respect to the density $\rho(\mathbf{r})$, we arrive at the formulas of the Thomas–Fermi theory. However, as noted earlier, this theory does not provide a good description of the properties of crystals under normal pressure, and the reason is that the local approximation (2.4) can be applied to systems with an electron number density that only slightly varies in space, which really is not the case with crystals. As noted by Kohn and Sham [18], the most serious difficulty with the local approximation is related to the kinetic energy. In their paper, Kohn and Sham proposed a procedure for removing this difficulty: they suggested looking for the solution of equation (2.1) for the density $\rho(\mathbf{r})$ in the form of the density of a certain system of noninteracting electrons placed in an external self-consistent field:

$$\rho(\mathbf{r})=\sum_i\left|\psi_i(\mathbf{r})\right|^2. \tag{2.5}$$

Here, for the wave functions $\psi_i(\mathbf{r})$ we can write an equation of the Schrödinger type [18],

$$\left[-\frac{\hbar^2\nabla^2}{2m}+V_{\rm eff}(\mathbf{r})\right]\psi_i=\varepsilon_i\psi_i\,, \tag{2.6}$$

where $V_{\rm eff}(\mathbf{r})$ is the effective potential of the form

$$V_{\rm eff}(\mathbf{r})=V_{\rm ext}+e^2\int\frac{\rho(\mathbf{r}')}{|\mathbf{r}-\mathbf{r}'|}\,{\rm d}\mathbf{r}'+V_{\rm xc}(\mathbf{r})\,, \tag{2.7}$$

and the exchange-correlation potential $V_{\rm xc}$ is given by the formula

$$V_{\rm xc}(\mathbf{r})=\frac{\delta E_{\rm xc}\{\rho(\mathbf{r}\}}{\delta\rho(\mathbf{r})}\,, \tag{2.8}$$

with the exchange correlation energy $E_{\rm xc}\{\rho(\mathbf{r})\}$ incorporating the contributions from the potential energy and the kinetic energy [see equation (2.2)].

In the literature, equation (2.6) is usually called the Kohn–Sham equation. If we now use the local approximation for the exchange-correlation energy,

$$\varepsilon_{\rm xc}\{\rho(\mathbf{r})\}=f\left[\rho(\mathbf{r})\right], \tag{2.9}$$

where the function $f\left[\rho(\mathbf{r})\right]$ is determined by the properties of the homogeneous interacting electron gas, the problem of calculating the electron number density in the crystal and the crystal's energy in the ground state is fully determined by the above system of equations. Many attempts have been made to improve the local approximation for the exchange-correlation energy by, say, introducing gradient correction terms. Here, however, we will not dwell on this problem any further — the interested reader can turn to a recent review by

Perdew and Kurth [20], where these problems are discussed in detail. Note that already within the local approximation many physical properties of crystals, including crystals with ionic bonds, are described with very good accuracy.

From the 1970s on, the density functional theory has been used in a number of calculations of properties of ionic crystals, including oxides with the perovskite structure [21–23]. Among other things, it was found that the energy of the distorted ferroelectric phase in $BaTiO_3$ and $PbTiO_3$ crystals is lower than the energy of the cubic phase, while in the $SrTiO_3$ crystal the phase with what is known as antiferrodistortions proves to be energy-preferable. Unfortunately, these calculations do not provide a clear picture of the physical reasons for a particular instability of the cubic phase. At the same time, within phenomenological theories of ionic crystals, the nature of, say, ferroelectric instability has been thoroughly established and amounts to a large negative (in sign) contribution to the energy of polar-active phonon modes of long-range dipole–dipole interactions between ions (for details see the review article in Ref. [16]). In the density functional theory described above there is no concept of ions and dipoles on ions: there is only a periodic distribution of electron density, which is defined as the sum (2.5) over the Bloch wave functions. Moreover, serious difficulties arise in this approach when one attempts to describe the phenomenon of electric polarization of an ionic crystal [24], and these difficulties led to the conclusion (see Ref. [25]) that all classical theories of ionic crystals are erroneous. Resta [25] states that in a crystal there can be no well-defined ions (with the result that the very notion of polarization of crystals as a sum of dipole moments on individual ions carries no physical meaning) and that polarization of a crystal is determined by the passage of current through it rather than by the redistribution of electron charge.

It is a well-known fact (see, e.g., Ref. [26]) that the macroscopic polarization vector $\mathbf{P}$ of a finite body is the average of the polarization density field $\mathbf{p}(\mathbf{r})$:

$$\mathbf{P} = \int \mathrm{d}\mathbf{r}\, \mathbf{p}(\mathbf{r})\,. \tag{2.10}$$

The field $\mathbf{p}(\mathbf{r})$ satisfies the equation [26]

$$\operatorname{div} \mathbf{p}(\mathbf{r}) = -\rho(\mathbf{r})\,, \tag{2.11}$$

where $\rho(\mathbf{r})$ is the total charge density. Obviously, the polarization $\mathbf{p}(\mathbf{r})$ exists only inside the body. Combining equations (2.10) and (2.11) and integrating (2.10) by parts, we get

$$\mathbf{P} = \int \mathbf{r}\rho(\mathbf{r})\, \mathrm{d}\mathbf{r} + \int_S \big(\mathbf{p}(\mathbf{r}) \cdot \mathrm{d}\mathbf{S}\big)\mathbf{r}\,. \tag{2.12}$$

The integration area S in (2.12) can be chosen to lie outside the body, but then the second term on the right-hand side of (2.12) is zero. Thus, the macroscopic polarization of a finite sample is uniquely determined by the sample's dipole moment, i.e., the first term on the right-hand side of (2.12).

The dipole moment of an electroneutral system with a periodic distribution of the charge density depends on how the sample was cut out, the state of its surface, and other factors, so that a direct generalization of (2.12) to an infinite sample is impossible [27]. Furthermore, the absolute value of polarization cannot be determined either theoretically or experimentally [28, 29]. The most that can be done is to measure the change in polarization caused by external agents of some sort, such as an external electric field, or by variations in the internal state of the crystal caused by, say, a ferroelectric phase transition from a nonpolar phase. These variations are determined by the bulk properties, and the part in the polarization related to them can be determined, at least theoretically, for an infinite sample. To this end one must take not the full polarization $\mathbf{P}$ but its variation $\Delta\mathbf{P}$. It has proven convenient to break down the change in polarization into two contributions, that from the displacement of atomic nuclei and the electron contribution:

$$\Delta\mathbf{P} = \Delta\mathbf{P}_{\mathrm{nucl}} + \Delta\mathbf{P}_{\mathrm{el}}\,. \tag{2.13}$$

In the case of a ferroelectric transition, the atomic-nuclei contribution is defined as follows [9]:

$$\Delta\mathbf{P}_{\mathrm{nucl}} = \frac{1}{v_0}\,\Delta\mathbf{d}_{\mathrm{nucl}} = \frac{1}{v_0}\sum_s Z^{\mathrm{nucl}}(s)\Delta\mathbf{R}(s)\,, \tag{2.14}$$

where v_0 is the unit-cell volume, $Z^{\mathrm{nucl}}(s)$ and $\Delta\mathbf{R}(s)$ are, respectively, the charge and displacement of the sth nucleus, and the sum in (2.14) is over one unit cell. The electron contribution to polarization is given by the expression [30, 31]

$$\Delta\mathbf{P}_{\mathrm{el}} = \frac{1}{v_0}\int_{v_0} \delta\mathbf{p}_{\mathrm{el}}(\mathbf{r})\, \mathrm{d}\mathbf{r}\,, \tag{2.15}$$

with $\delta\mathbf{p}_{\mathrm{el}}(\mathbf{r})$ satisfying the equation

$$\operatorname{div} \delta\mathbf{p}_{\mathrm{el}}(\mathbf{r}) = -\delta\rho_{\mathrm{el}}(\mathbf{r})\,, \tag{2.16}$$

where $\delta\rho_{\mathrm{el}}(\mathbf{r})$ is the change in the electron density related to the displacement of nuclei. Now, integrating equation (2.15) by parts, we can show (see Ref. [27]) that

$$\Delta\mathbf{P}_{\mathrm{el}} = \frac{1}{v_0}\int_{v_0} \mathbf{r}\,\delta\rho(\mathbf{r})\, \mathrm{d}\mathbf{r} + \frac{1}{v_0}\int_S \mathbf{r}(\mathbf{n}\cdot\delta\mathbf{p}_{\mathrm{el}})\, \mathrm{d}S\,. \tag{2.17}$$

The first term on the right-hand side of (2.17) together with the contribution (2.14) from nuclei displacement gives the unit-cell dipole moment, while the second term actually describes the charge transfer from one cell to another. The second term vanishes in the case of polarizable point ions [28, 29], with the result that the crystal polarization is the sum of the dipole moments of the unit cells. Note that in this case the polarization is independent of the choice of the unit cell. But when the electron charge is distributed continuously, as is the case with crystals, we simply do not know what to do with the second term in (2.17), especially if we are calculating the homogeneous polarization of the crystal as a whole. In a fairly early work in this field of research, Bennett and Maradudin [32] calculated the electron contribution to the change in polarization of crystals with a zinc-blende structure caused by sublattice shifts by d. The researchers used in their calculations only the first term in (2.17):

$$\delta\mathbf{P}_{\mathrm{el}} = \lim_{d\to 0}\frac{1}{d}\int_{v_0} \mathbf{d}\cdot\mathbf{r}\big[\rho(\mathbf{r}) - \rho_0(\mathbf{r})\big]\, \mathrm{d}\mathbf{r}\,, \tag{2.18}$$

where $\mathbf{d}$ is the unit vector characterizing the shift of the sublattices. The distribution of electron density in the distorted, $\rho(\mathbf{r})$, and undistorted, $\rho_0(\mathbf{r})$, crystals were calcu-

lated by the density functional method within the pseudopotential approach. Their results (see Ref. [32]) were found to agree very well with the experimental data. However, their approach was criticized severely by Resta [24, 25] and Martin [27], who believed such agreement to be purely coincidental.

As noted earlier, a direct generalization of expression (2.12) for the polarization of finite bodies to the case of an infinite crystal, which is defined by periodic boundary conditions, is impossible. The essence of this difficulty is as follows. Let us write the expectation value of the position operator x, where

$$x = \sum_{i=1}^{N} x_i \,, \tag{2.19}$$

as

$$\langle \psi_0 | x | \psi_0 \rangle = \int x \rho(x) \, \mathrm{d}x \,. \tag{2.20}$$

When periodic boundary conditions

$$\psi_0(x + L) = \psi_0(x) \tag{2.21}$$

are imposed, the operator x does not commute with the operator of a shift by L, with the result that the expectation value in (2.20) cannot be determined [33]. In the early 1990s, a new approach to determining the polarization of a periodic crystal was proposed by Resta [34] and King-Smith and Vanderbilt [35]. It was based on the following definition of polarization:

$$\frac{\partial \mathbf{P}_{\mathrm{el}}(\mathbf{r}, t)}{\partial t} = \mathbf{j}_{\mathrm{el}}(\mathbf{r}, t) \,. \tag{2.22}$$

The validity of this definition can easily be proved if we use equation (2.11) and the continuity equation

$$\operatorname{div} \mathbf{j}_{\mathrm{el}}(\mathbf{r}, t) + \frac{\partial \rho_{\mathrm{el}}(\mathbf{r}, t)}{\partial t} = 0 \,. \tag{2.23}$$

Expressing (2.22) in terms of the Fourier transforms $\mathbf{P}_{\mathrm{el}}(\mathbf{q}, \omega)$ and $\mathbf{j}_{\mathrm{el}}(\mathbf{q}, \omega)$, we arrive at

$$\mathbf{P}_{\mathrm{el}}(\mathbf{q}, \omega) = -\mathrm{i} \, \frac{\mathbf{j}_{\mathrm{el}}(\mathbf{q}, \omega)}{\omega} \,. \tag{2.24}$$

In the adiabatic approximation $\omega \to 0$, the expression for the static uniform polarization assumes the form

$$\mathbf{P}_{\mathrm{el}} = \lim_{\omega \to 0} \left[\lim_{\mathbf{q} \to 0} \operatorname{Im} \frac{\mathbf{j}_{\mathrm{el}}(\mathbf{q}, \omega)}{\omega} \right] . \tag{2.25}$$

In contrast to the position operator, the current operator is a well-defined quantity and its expectation value over the quantum mechanical state of the system, including the case of a crystal with periodic boundary conditions, can easily be calculated. To this end we write the Kohn – Sham equation (2.6) for a periodic crystal in the form

$$\left[-\frac{\hbar^2 \nabla^2}{2m} + V_{\mathrm{eff}}(\mathbf{r}) \right] \psi_{\mathbf{k}n}(\mathbf{r}) = \varepsilon_{\mathbf{k}n} \psi_{\mathbf{k}n}(\mathbf{r}) \,, \tag{2.26}$$

where the $\psi_{\mathbf{k}n}(\mathbf{r})$ are the Bloch wave functions

$$\psi_{\mathbf{k}n}(\mathbf{r}) = \exp(\mathrm{i}\mathbf{k}\mathbf{r}) \, u_{\mathbf{k}n}(\mathbf{r}) \,, \tag{2.27}$$

with $u_{\mathbf{k}n}(\mathbf{r})$ the Bloch amplitude, which is periodic in $\mathbf{r}$, and n the band index. Now let us examine a change in the electron polarization of the crystal caused by an adiabatic change in the self-consistent Kohn – Sham potential. We can parameterize the variation of the potential by a variable λ, where $\lambda = 0$ corresponds to the initial state of the system and $\lambda = 1$ to the final state. The full variation of polarization in this process can be written as follows:

$$\Delta \mathbf{P}_{\mathrm{el}} = \int_0^1 \frac{\partial \mathbf{P}}{\partial \lambda} \, \mathrm{d}\lambda \,. \tag{2.28}$$

In perturbation theory, the variation of the current passing through the system that is caused by a small variation in λ can be written as

$$\frac{\partial j_x}{\partial \lambda} = \frac{2e}{v} \sum_{\mathbf{k}} \sum_{n} \left\langle \psi_{\mathbf{k}n}^{(\lambda)}(\mathbf{r}) | j_x | \, \frac{\partial \psi_{\mathbf{k}n}^{(\lambda)}(\mathbf{r})}{\partial \lambda} \right\rangle , \tag{2.29}$$

where v is the crystal volume, the sum is over filled bands, and j_x is the x-component of the current operator, or

$$j_x = -\frac{\mathrm{i}\hbar}{m} \nabla_x \,. \tag{2.30}$$

The change in the wave function $\partial \psi_{\mathbf{k}n}^{(\lambda)}(\mathbf{r}) / \partial \lambda$ can be expressed in the following manner:

$$\frac{\partial \psi_{\mathbf{k}n}^{(\lambda)}(\mathbf{r})}{\partial \lambda} = \sum_{m \neq n} \psi_{\mathbf{k}m} \left\langle \psi_{\mathbf{k}m} \left| \frac{\partial V_{\mathrm{eff}} / \partial \lambda}{\varepsilon_{\mathbf{k}n} - \varepsilon_{\mathbf{k}m}} \right| \psi_{\mathbf{k}n} \right\rangle . \tag{2.31}$$

Integration under the averaging sign $\langle \, \rangle$ in (2.29) and (2.31) is done over the entire crystal. Plugging (2.31) into (2.29) and using (2.25), we can show (see Ref. [35]) that in the adiabatic limit $\partial P_x / \partial \lambda$ has the form

$$\frac{\partial P_x}{\partial \lambda} = \frac{2e}{v} \operatorname{Im} \sum_{\mathbf{k}} \sum_{n=1}^{M} \sum_{m=M+1}^{\infty} \frac{\langle \psi_{\mathbf{k}n}^{\lambda} | j_x | \psi_{\mathbf{k}m}^{\lambda} \rangle \langle \psi_{\mathbf{k}m}^{\lambda} | \partial V_{\mathrm{eff}}^{\lambda} / \partial \lambda | \psi_{\mathbf{k}n}^{\lambda} \rangle}{(\varepsilon_{\mathbf{k}n}^{\lambda} - \varepsilon_{\mathbf{k}m}^{\lambda})^2} \,. \tag{2.32}$$

We can write this expression in a form in which summation is done only over filled bands, similar to the way it was done by Thouless et al. [36] for the quantum Hall effect, if we allow for

$$\langle \psi_{\mathbf{k}n}^{\lambda} | j_x | \psi_{\mathbf{k}m}^{\lambda} \rangle = \left\langle u_{\mathbf{k}n}^{\lambda} \left| \left[\sum \frac{\partial}{\partial k_x} \, , H_{\mathbf{k}\lambda} \right] \right| u_{\mathbf{k}m}^{\lambda} \right\rangle \tag{2.33}$$

and

$$\left\langle \psi_{\mathbf{k}m}^{\lambda} \left| \frac{\partial V_{\mathrm{eff}}^{\lambda}}{\partial \lambda} \right| \psi_{\mathbf{k}n}^{\lambda} \right\rangle = \left\langle u_{\mathbf{k}n}^{\lambda} \left| \left[\frac{\partial}{\partial \lambda} \, , H_{\mathbf{k}\lambda} \right] \right| u_{\mathbf{k}m}^{\lambda} \right\rangle . \tag{2.34}$$

Here, $H_{\mathbf{k}\lambda}$ is the Hamiltonian:

$$H_{\mathbf{k}\lambda} = \frac{1}{2m} (-\mathrm{i}\hbar\nabla + \hbar\mathbf{k})^2 + V_{\mathrm{eff}}^{\lambda}(\mathbf{r}) \,. \tag{2.35}$$

Plugging (2.33) – (2.35) into (2.32), we arrive at the following expression for the polarization's change ΔP_x:

$$\Delta P_x = \frac{2e}{(2\pi)^3} \operatorname{Im} \sum_{n=1}^{M} \int \mathrm{d}^3 k \int_0^1 \mathrm{d}\lambda \left[\left\langle \frac{\partial u_{\mathbf{k}n}^{\lambda}}{\partial k_x} \left| \frac{\partial u_{\mathbf{k}n}^{\lambda}}{\partial \lambda} \right\rangle \right. \right. \\ \left. \left. - \left\langle \frac{\partial u_{\mathbf{k}n}^{\lambda}}{\partial \lambda} \left| \frac{\partial u_{\mathbf{k}n}^{\lambda}}{\partial k_x} \right\rangle \right] \right. , \tag{2.36}$$

where the integral with respect to momentum is evaluated within the first Brillouin zone. Integrating by parts, we get

$$\Delta P_x = \frac{2e}{(2\pi)^3}\ \mathrm{Im}\sum_{n=1}^{M}\int \mathrm{d}^3k\left[\left\langle u^{\lambda}_{\mathbf{k}n}\middle|\frac{\partial}{\partial k_x}\middle|u^{\lambda}_{\mathbf{k}m}\right\rangle\right|_0^1 - \int_0^1 \mathrm{d}\lambda\ \frac{\partial}{\partial k_x}\left\langle u^{\lambda}_{\mathbf{k}n}\middle|\frac{\partial}{\partial\lambda}\middle|u^{\lambda}_{\mathbf{k}n}\right\rangle\right]. \tag{2.37}$$

Since the function $u^{\lambda}_{\mathbf{k}n}$ can be chosen in the form of a periodic function in $\mathbf{k}$, the second term in (2.37) vanishes, and we arrive at the well-known two-point function for ΔP_x (see Refs [24, 25, 35]):

$$\Delta P_x = P_x^{\lambda} - P_x^0\,, \tag{2.38}$$

where

$$P_x^{\lambda} = \frac{2e}{(2\pi)^3}\ \mathrm{Im}\sum_{n=1}^{M}\int \mathrm{d}^3k\left\langle u^{\lambda}_{\mathbf{k}n}\middle|\frac{\partial}{\partial k_x}\middle|u^{\lambda}_{\mathbf{k}n}\right\rangle. \tag{2.39}$$

The integral on the right-hand side of (2.39) is closely linked to what is known as the Berry phase [37] for the nth band.

Here, we will not dwell any further on the relation of the Berry phase with the electron polarization and the method used to calculate the crystal polarization within the given approach. The interested reader can find all this in Resta's detailed review [25]. It would seem that the above expressions for the electron polarization, (2.38) and (2.39), fully corroborate the validity of the ideas (expressed, in particular, in Resta's review articles [24, 25]) that the polarization of a crystal is determined by the phase of the wave functions rather than by the redistribution of charge density. If we assume that the Bloch amplitudes are real-valued functions, polarization is zero, in agreement with (2.39). On the other hand, it is generally accepted that the charge density is determined by the absolute value of the wave function and does not depend on the wave function's phase. Actually, the situation is not so simple. The periodic density in the crystal also has a certain phase, which depends on the boundary conditions. Let us discuss this problem in greater detail using, for this purpose, the results of Kvyatkovskiĭ's research [30, 31, 38]. We go back to (2.17) to examine the derivation of this formula in a more consistent approach, based on the long-wavelength method [9], although earlier this formula was derived directly for a homogeneous polarization of the crystal. Clearly, the redistribution of the electron density, $\delta\rho_{\mathrm{el}}(\mathbf{r})$, caused by a small variation in the parameters of the Kohn–Sham Hamiltonian, satisfies the electroneutrality condition

$$\int \mathrm{d}\mathbf{r}\,\delta\rho_{\mathrm{el}}(\mathbf{r}) = 0\,. \tag{2.40}$$

Introducing the change $\delta\mathbf{p}_{\mathrm{el}}(\mathbf{r})$ in the polarization field, we can, using equation (2.16), define the Fourier transforms $\delta\rho_{\mathrm{el}}(\mathbf{q})$ and $\delta\mathbf{p}_{\mathrm{el}}(\mathbf{q})$ as follows:

$$\begin{aligned}\delta\rho_{\mathrm{el}}(\mathbf{q}) &= \frac{1}{v}\int \mathrm{d}\mathbf{r}\,\exp(-\mathrm{i}\mathbf{q}\mathbf{r})\,\delta\rho_{\mathrm{el}}(\mathbf{r})\,,\\ \delta\mathbf{p}_{\mathrm{el}}(\mathbf{q}) &= \frac{1}{v}\int \mathrm{d}\mathbf{r}\,\exp(-\mathrm{i}\mathbf{q}\mathbf{r})\,\delta\mathbf{p}_{\mathrm{el}}(\mathbf{r})\,.\end{aligned} \tag{2.41}$$

Equation (2.16) then yields

$$\delta\rho_{\mathrm{el}}(\mathbf{q}) = -\mathrm{i}\left[\mathbf{q}\cdot\delta\mathbf{p}_{\mathrm{el}}(\mathbf{q}) + O(q^2)\right]. \tag{2.42}$$

Now in equation (2.41) we can pass from integration over the entire volume of the crystal to summation over the Bravais lattice and integration over unit-cell volume and represent $\delta\rho_{\mathrm{el}}(\mathbf{q})$ in the form

$$\delta\rho_{\mathrm{el}}(\mathbf{q}) = \frac{1}{v_0}\int_{v_0}\mathrm{d}\mathbf{r}\,\exp(-\mathrm{i}\mathbf{q}\mathbf{r})\,\delta\rho_{\mathrm{el}}(\mathbf{r};\mathbf{q})\,, \tag{2.43}$$

where

$$\delta\rho_{\mathrm{el}}(\mathbf{r};\mathbf{q}) = \frac{1}{N}\sum_{\mathbf{R}}\exp(-\mathrm{i}\mathbf{q}\mathbf{R})\,\delta\rho_{\mathrm{el}}(\mathbf{r}+\mathbf{R})\,, \tag{2.44}$$

with N the number of unit cells. In (2.43) and (2.44), $\mathbf{r}$ varies within a single unit cell, with the result that we have the following expansion of $\delta\rho_{\mathrm{el}}(\mathbf{q})$ for small $\mathbf{q}$'s:

$$\delta\rho_{\mathrm{el}}(\mathbf{q}) = \frac{1}{v_0}\,\delta Q_{\mathrm{el}}(\mathbf{q}) - \mathrm{i}\,\frac{1}{v_0}(\mathbf{q}\cdot\delta\mathbf{d}_{\mathrm{el}}) + O(q^2)\,, \tag{2.45}$$

where

$$\delta Q_{\mathrm{el}}(\mathbf{q}) = \int_{v_0}\delta\rho_{\mathrm{el}}(\mathbf{r};\mathbf{q})\,\mathrm{d}\mathbf{r} \tag{2.46}$$

and $\delta\mathbf{d}_{\mathrm{el}}$ is the unit-cell dipole moment equal to

$$\delta\mathbf{d}_{\mathrm{el}} = \lim_{\mathbf{q}\to 0}\int_{v_0}\mathbf{r}\,\delta\rho_{\mathrm{el}}(\mathbf{r};\mathbf{q})\,\mathrm{d}\mathbf{r}\,. \tag{2.47}$$

Actually, we have arrived at (2.17). Now we need only to prove, using the Kohn–Sham equation, that $\delta Q_{\mathrm{el}}(\mathbf{q})$ tends to zero like $\mathbf{q}^2$ as $\mathbf{q}\to 0$. In this case, the change in the electron polarization, $\delta\mathbf{p}_{\mathrm{el}}(\mathbf{q})$, is given, as $\mathbf{q}\to 0$, in accordance with (2.42) and (2.47), by the formula

$$\delta\mathbf{p}_{\mathrm{el}} = \delta\mathbf{d}_{\mathrm{el}} = \int_{v_0}\mathbf{r}\,\delta\rho_{\mathrm{el}}(\mathbf{r})\,\mathrm{d}\mathbf{r}\,. \tag{2.48}$$

The use of the long-wavelength method makes it possible to ignore the ill-defined position operator $\mathbf{r}$ in the entire volume of the crystal, since integration is now carried out over a unit cell. By analogy with the above calculations, we can write the following expression for the current variation under an adiabatic variation of the self-consistent potential [equations (2.29)–(2.31)]:

$$\frac{\partial}{\partial\lambda}\,Q^{\lambda}_{\mathrm{el}}(\mathbf{q}) = \frac{2e}{v}\sum_{n,m,\mathbf{k}}\left(A^{\lambda}_{m\mathbf{k},\,n\mathbf{k}+\mathbf{q}}\left\langle\psi^{\lambda}_{n\mathbf{k}+\mathbf{q}}\middle|\frac{\partial}{\partial\lambda}\middle|\psi^{\lambda}_{m\mathbf{k}}\right\rangle - A^{\lambda}_{n\mathbf{k},\,m\mathbf{k}+\mathbf{q}}\left\langle\psi^{\lambda}_{m\mathbf{k}+\mathbf{q}}\middle|\frac{\partial}{\partial\lambda}\middle|\psi^{\lambda}_{n\mathbf{k}}\right\rangle\right), \tag{2.49}$$

where

$$A^{\lambda}_{m\mathbf{k},\,n\mathbf{k}+\mathbf{q}} = (\psi^{\lambda}_{m\mathbf{k}}|\psi^{\lambda}_{n\mathbf{k}+\mathbf{q}}) = \left(u^{\lambda}_{m\mathbf{k}}\middle|\exp(\mathrm{i}\mathbf{q}\mathbf{r})\middle|u^{\lambda}_{n\mathbf{k}+\mathbf{q}}\right) \tag{2.50}$$

and we have introduced the notation

$$\langle A|B\rangle = \frac{1}{v}\int_{v}\mathrm{d}\mathbf{r}\,A^*(\mathbf{r})B(\mathbf{r})\,, \tag{2.51}$$

$$(A|B) = \frac{1}{v_0}\int_{v_0}\mathrm{d}\mathbf{r}\,A^*(\mathbf{r})B(\mathbf{r})\,. \tag{2.52}$$

Integration in (2.51) is carried out over the entire crystal volume and in (2.52) over the unit-cell volume. For regions where the $\mathbf{q}$'s are small we can write $A^{\lambda}_{m\mathbf{k},\,n\mathbf{k}+\mathbf{q}}$ in the form

$$A^{\lambda}_{m\mathbf{k},\,n\mathbf{k}+\mathbf{q}} = \delta_{mn} + \mathbf{q}S^{\lambda}_{m\mathbf{k},\,n\mathbf{k}} + O(q^2)\,. \tag{2.53}$$

It can also be shown (see Ref. [31]) that

$$S^{\lambda}_{m\mathbf{k},\,n\mathbf{k}} = \delta_{mn}\,. \tag{2.54}$$

This implies that

$$\frac{\partial}{\partial\lambda}\,Q^{\lambda}_{\mathrm{el}}(\mathbf{q}) \approx O(q^2) \tag{2.55}$$

and that the change in the electron polarization, $\partial\mathbf{p}^{\lambda}_{\mathrm{el}}/\partial\lambda$, is determined by change in the dipole moment, $\partial\mathbf{d}_{\mathrm{el}}(\lambda)/\partial\lambda$. In turn, this quantity, in accordance with equation (2.48), is given by the expression

$$\frac{\partial}{\partial\lambda}\,\mathbf{d}_{\mathrm{el}}(\lambda) = \int \mathbf{r}\,\frac{\partial\bigl[\delta\rho_{\mathrm{el}}(\mathbf{r},\lambda)\bigr]}{\partial\lambda}\,\mathrm{d}\mathbf{r}\,. \tag{2.56}$$

Using the wave functions of the Kohn – Sham equation and their variation with the parameter λ, we can write (2.56) in another way:

$$\frac{\partial}{\partial\lambda}\,\mathbf{d}_{\mathrm{el}}(\lambda) = -\frac{2e}{v_0}\sum_{n,m,\mathbf{k}}\left\{(u^{\lambda}_{n\mathbf{k}}|\mathbf{r}|u^{\lambda}_{m\mathbf{k}})\left(u^{\lambda}_{m\mathbf{k}}\left|\frac{\partial}{\partial\lambda}\right|u^{\lambda}_{n\mathbf{k}}\right) + \text{c.c.}\right\}. \tag{2.57}$$

Allowing for the fact that

$$(u^{\lambda}_{n\mathbf{k}}|\mathbf{r}|u^{\lambda}_{m\mathbf{k}}) = \mathrm{i}\left(u^{\lambda}_{n\mathbf{k}}\left|\frac{\partial}{\partial\mathbf{k}}u^{\lambda}_{m\mathbf{k}}\right.\right), \tag{2.58}$$

we can write the expression for the change in electron polarization as follows:

$$\frac{\partial}{\partial\lambda}\,\delta\mathbf{p}^{\lambda}_{\mathrm{el}} = \frac{2e}{v_0}\,\mathrm{Im}\sum_{n,m,\mathbf{k}}\left\{\left(\frac{\partial}{\partial k}u^{\lambda}_{n\mathbf{k}}\left|\frac{\partial}{\partial\lambda}u^{\lambda}_{n\mathbf{k}}\right.\right) - \left(\frac{\partial}{\partial\lambda}u^{\lambda}_{n\mathbf{k}}\left|\frac{\partial}{\partial\mathbf{k}}u^{\lambda}_{n\mathbf{k}}\right.\right)\right\}. \tag{2.59}$$

Thus, we have arrived at the same expression that is derived by Resta [24, 25, 34] and King-Smith and Vanderbilt [35]. This means, for one thing, that the definition of the nature of electron polarization given in classical textbooks on solid state physics is meaningful and that the good agreement between theory and experiment achieved by Bennett and Maradudin [32] for the crystals with a zinc-blende structure is hardly accidental. The use of the Berry phase in describing polarization processes in crystals is simply the use of another mathematical tool and not a transition to new physics. Unfortunately, after the harsh criticism of Bennett and Maradudin's paper, researchers engaged in first-principles calculations of the properties of crystals made no attempt to repeat such calculations for crystals with other structures, while such attempts would make a lot of sense. However, it must be noted at this point, as was done by Kvyatkovskiĭ [31, 38], that formula (2.48) describing the change in electron polarization is sure to become invalid for an arbitrary periodic density distribution. But the quantum-mechanical calculation of the change in charge density for the same selection of unit cell makes it possible to correctly describe such a change in polarization.

3. The polarizable and deformable ion model

In the previous section we examined a method for calculating the electron polarization for insulator crystals of any type. The method is based on solving the Kohn – Sham equation in order to obtain periodic wave functions and their changes caused by variations of the parameters of the system or by applying external fields to the system. In the present section we deal with a dramatically different approach, also based on the first-principles calculations of the equilibrium properties, the electric polarization, and the lattice dynamics of ionic crystals. The approach uses a representation of the crystal's electron density in the form of a sum of the densities of individual overlapping ions (rather than the density of a system of noninteracting electrons placed in a self-consistent periodic potential):

$$\rho(\mathbf{r}) = \sum_i \rho_i(\mathbf{r} - \mathbf{R}_i)\,. \tag{3.1}$$

Such an approach was used in the already cited work by Jensen and Lenz [1]. The density functional method, combined with expression (3.1) for the electron density, was used by Kim and Gordon [39] in their calculation of the properties of ionic crystals. The researchers used the Hartree – Fock method to calculate the electron density $\rho_i(\mathbf{r} - \mathbf{R}_i)$ of an individual ion. They also assumed that this density does not change when the crystal is formed, which corresponds to the rigid ion model. In this case, the total energy of the crystal can be written as follows:

$$E^{\mathrm{cr}} = E\left\{\sum_i \rho_i(\mathbf{r} - \mathbf{R}_i)\right\} + E^{\mathrm{N}}\,, \tag{3.2}$$

where

$$E^{\mathrm{N}} = \frac{1}{2}\sum_{i,i'}\frac{Z^{\mathrm{N}}_i Z^{\mathrm{N}}_{i'}}{|\mathbf{R}_i - \mathbf{R}_{i'}|}\,, \tag{3.3}$$

with Z^{N}_i being the nuclear charge.

The quantity $E\{\rho(\mathbf{r})\}$ is the electron density functional and assumes the form

$$E\{\rho(\mathbf{r})\} = \int \mathrm{d}\mathbf{r}\,\rho(\mathbf{r})V_{\mathrm{ext}}(\mathbf{r}) + \frac{1}{2}\int \mathrm{d}\mathbf{r}\,\mathrm{d}\mathbf{r}'\,\frac{\rho(\mathbf{r})\rho(\mathbf{r}')}{|\mathbf{r} - \mathbf{r}'|} + \int \mathrm{d}\mathbf{r}\,F\{\rho(\mathbf{r})\}\,, \tag{3.4}$$

where $F\{\rho(\mathbf{r})\}$ is a universal density functional describing the contributions of the kinetic and exchange-correlation energies. Kim and Gordon [39] used the local Thomas – Fermi approximation [2, 3] for $F\{\rho(\mathbf{r})\}$. In order to improve the convergence of calculations, to the expression for the total energy we can add (and subtract) the sum of energies of individual ions:

$$E^{\mathrm{cr}} = \left[E\left\{\sum_i \rho_i(\mathbf{r} - \mathbf{R}_i)\right\} - \sum_i E\{\rho_i(\mathbf{r} - \mathbf{R}_i)\}\right] + \sum_i E\{\rho_i(\mathbf{r} - \mathbf{R}_i)\} + E^{\mathrm{N}}\,. \tag{3.5}$$

Ignoring the overlap of more than two ions immediately and the self-energies of ions added in (3.5), we can write (3.5) in the form

$$E^{\mathrm{cr}} = \frac{1}{2}\sum_{i\neq i'} \frac{Z_i^{\mathrm{N}} Z_{i'}^{\mathrm{N}}}{|\mathbf{R}_i - \mathbf{R}_{i'}|} + \frac{1}{2}\sum_{i\neq i'} V_{i,i'}\,, \tag{3.6}$$

where

$$V_{i,i'} = E\{\rho_i(\mathbf{r}-\mathbf{R}_i) + \rho_{i'}(\mathbf{r}-\mathbf{R}_{i'})\} - E\{\rho_i(\mathbf{r}-\mathbf{R}_i)\} - E\{\rho_{i'}(\mathbf{r}-\mathbf{R}_{i'})\}\,. \tag{3.7}$$

Now, if we use (3.4), we can write

$$\begin{aligned} V_{i,i'} = {} & \int \mathrm{d}\mathbf{r}\, \rho_i(\mathbf{r}-\mathbf{R}_i)\frac{Z_{i'}^{\mathrm{N}}}{|\mathbf{r}-\mathbf{R}_{i'}|} + \int \mathrm{d}\mathbf{r}\, \rho_{i'}(\mathbf{r}-\mathbf{R}_{i'})\frac{Z_i^{\mathrm{N}}}{|\mathbf{r}-\mathbf{R}_i|} \\ & + \frac{1}{2}\int \mathrm{d}\mathbf{r} \int \mathrm{d}\mathbf{r}'\, \frac{\rho_i(\mathbf{r}-\mathbf{R}_i)\,\rho_{i'}(\mathbf{r}-\mathbf{R}_{i'})}{|\mathbf{r}-\mathbf{r}'|} \\ & + \int \mathrm{d}\mathbf{r}\, \big[F\{\rho_i(\mathbf{r}-\mathbf{R}_i) + \rho_{i'}(\mathbf{r}-\mathbf{R}_{i'})\} \\ & - F\{\rho_i(\mathbf{r}-\mathbf{R}_i)\} - F\{\rho_{i'}(\mathbf{r}-\mathbf{R}_{i'})\}\big]\,. \end{aligned} \tag{3.8}$$

Next, we introduce the quantity Z_i^{el}, which is the total number of electrons on a given ion:

$$Z_i^{\mathrm{el}} = \int \mathrm{d}\mathbf{r}\, \rho_i(\mathbf{r})\,. \tag{3.9}$$

Thus,

$$Z_i^{\mathrm{N}} + Z_i^{\mathrm{el}} = Z_i^{\mathrm{ion}}\,, \tag{3.10}$$

where Z_i^{ion} is the charge of the respective ion. Adding (and then subtracting) the quantity $Z_i^{\mathrm{el}}\delta(\mathbf{r}-\mathbf{R}_i)$ in the first two terms on the right-hand side of (3.8), we can write the expression for the crystal energy in the form

$$E^{\mathrm{cr}} = E^{\mathrm{M}} + \frac{1}{2}\sum_{i\neq i'} \tilde{V}_{i,i'}\,. \tag{3.11}$$

Here, E^{M} is the Madelung energy of point ions:

$$E^{\mathrm{M}} = \frac{1}{2}\sum_{i\neq i'} \frac{Z_i^{\mathrm{ion}} Z_{i'}^{\mathrm{ion}}}{|\mathbf{R}_i - \mathbf{R}_{i'}|}\,. \tag{3.12}$$

For $\tilde{V}_{i,i'}$ we can write the following expression:

$$\begin{aligned} \tilde{V}_{i,i'} = {} & \int \mathrm{d}\mathbf{r}\, \big[\rho_i(\mathbf{r}-\mathbf{R}_i) - Z_i^{\mathrm{el}}\delta(\mathbf{r}-\mathbf{R}_i)\big]\frac{Z_{i'}^{\mathrm{N}}}{|\mathbf{r}-\mathbf{R}_{i'}|} \\ & + \int \mathrm{d}\mathbf{r}\, \big[\rho_{i'}(\mathbf{r}-\mathbf{R}_{i'}) - Z_{i'}^{\mathrm{el}}\delta(\mathbf{r}-\mathbf{R}_{i'})\big]\frac{Z_i^{\mathrm{N}}}{|\mathbf{r}-\mathbf{R}_i|} \\ & + \frac{1}{2}\int \mathrm{d}\mathbf{r} \int \mathrm{d}\mathbf{r}'\, \frac{1}{|\mathbf{r}-\mathbf{r}'|}\big[\rho_i(\mathbf{r}-\mathbf{R}_i) - Z_i^{\mathrm{el}}\delta(\mathbf{r}-\mathbf{R}_i)\big] \\ & \times \big[\rho_{i'}(\mathbf{r}-\mathbf{R}_{i'}) - Z_{i'}^{\mathrm{el}}\delta(\mathbf{r}-\mathbf{R}_{i'})\big] \\ & + \int \mathrm{d}\mathbf{r}\, \big[F\{\rho_i(\mathbf{r}-\mathbf{R}_i) + \rho_{i'}(\mathbf{r}-\mathbf{R}_{i'})\} \\ & - F\{\rho_i(\mathbf{r}-\mathbf{R}_i)\} - F\{\rho_{i'}(\mathbf{r}-\mathbf{R}_{i'})\}\big]\,. \end{aligned} \tag{3.13}$$

The interaction $\tilde{V}_{i,i'}$ can be evaluated by computer-aided numerical methods and represents the short-range repulsion between ions.

Thus, the Kim–Gordon model in its original form is reduced, in accordance with (3.11), to the well-known rigid ion model [40]. The calculations done by Kim and Gordon [39] show that this model, which contains no adjustable parameters, provides a fairly good description of the static properties of alkali-halide crystals. However, like any rigid ion model, it has a number of drawbacks, since it completely ignores the difference in the charge density distributions of a free ion and an ion that is part of a crystal. The experimental data suggest that even in alkali-halide crystals the electron density on negative ions proves to be suppressed compared to the density of free ions [41]. When an external electric field is applied to the crystal, the induced dipole moments appear on the ions, which leads to dipole-type deformations of the electron density. In many ionic crystals, the presence of deformations of the quadrupole type in the electron density of ions may strongly affect the physical properties of the crystals. In addition, the Kim–Gordon model does not allow for calculations of some ionic crystals, e.g., oxides, since the oxygen ion O^{2-} does not exist in a vacuum and is stabilized only in the field of the crystalline environment.

The problem of using the Kim–Gordon model in calculating the properties of ionic crystals with ions that are unstable in a vacuum has been solved by a number of researchers [42–44], who have used the concept of a Watson sphere [45]. To calculate the electron density they proposed calculating it not for a free ion but for an ion surrounded by a charged sphere, whose potential has the form

$$V^{\mathrm{W}}(r) = \begin{cases} \dfrac{Z_i^{\mathrm{ion}}}{R_{\mathrm{W}}} & \text{for } r < R_{\mathrm{W}}\,, \\[2ex] \dfrac{Z_i^{\mathrm{ion}}}{r} & \text{for } r > R_{\mathrm{W}}\,, \end{cases} \tag{3.14}$$

where R_{W} is the radius of the Watson sphere. Solving the quantum mechanical equation for an ion with potential (3.14), we can find the charge density distribution for any value of R_{W}. A consistent approach to the choice of the radius R_{W} amounts to determining it from the minimum condition imposed on the total energy of the crystal. In solving this problem, Muhlhausen and Gordon [43] and Wolf and Bukowinski [44] met with serious difficulties. As shown above, to pass from formula (3.2) for the total energy of the crystal to formula (3.11), which is the total energy in the rigid ion model, one must subtract and add the sum of the energies of individual ions. In the Kim–Gordon approach, which uses the electron densities of free ions, one can ignore the added sum of ion energies and actually discard it, since it is independent of the crystalline environment. Things change dramatically when we include the potential of the Watson sphere in our picture. Hence, we should clearly understand what we are adding to and subtracting from the crystal energy (3.2), if the charge density depends on R_{W}. Similar difficulties were encountered in Ref. [46], where the possibility of dipole moments appearing on the ions was included in the picture. This problem can be consistently solved only by the methods developed by Leontovich [47] in his theory of nonequilibrium thermodynamics, and this was done in Refs [48–54]. The essence of our generalizations of the Kim–Gordon model amounts to the following. First, in accordance with Leontovich's theory of nonequilibrium thermodynamics [47], we

must prepare a nonequilibrium state for each individual electron density distribution, in which the ions posses a different multipole symmetry. This means that we must prepare ions characterized by a certain effective radius K_0, a dipole moment **p**, a quadrupole moment **Q**, etc. To this end, the Kohn–Sham equation for a separate ion is solved in the presence of auxiliary fields with the respective symmetries. The equation can be written as follows:

$$\left[-\frac{\hbar^2\nabla^2}{2m}+\frac{Z_i^{\mathrm{N}}}{|\mathbf{r}|}+\int \mathrm{d}\mathbf{r}'\,\frac{\rho_i(\mathbf{r}')}{|\mathbf{r}-\mathbf{r}'|}+V_{\mathrm{xc}}(\mathbf{r})+V_{\mathrm{ext}}(\mathbf{r},K_l)\right]\psi_\alpha(\mathbf{r}) = \varepsilon_\alpha\psi_\alpha(\mathbf{r})\,. \tag{3.15}$$

For the spherically symmetric part of the external field we take the potential (3.14) of a Watson sphere, while the potentials of higher multipoles are taken in the form

$$V_{\mathrm{ext}}(\mathbf{r},K_l) = -r^l K_l P_l(\cos\theta)\,. \tag{3.16}$$

In the case of dipole symmetry, K_l is simply the amplitude of the external electric field. Actually, to improve the procedure of numerical calculations in Ref. [53], we used smoother auxiliary potentials, but this is quite unimportant for our further discussion.

To solve equation (3.15), we used the perturbation technique proposed by Sternheimer [55] and wrote the wave function $\psi_\alpha(\mathbf{r})$ in the form

$$\psi_\alpha(\mathbf{r}) = \psi_\alpha^0(\mathbf{r}) + \delta\psi_\alpha(\mathbf{r}) \tag{3.17}$$

and

$$\delta\rho(\mathbf{r}) = 2\sum_\alpha \psi_\alpha^0(\mathbf{r})\,\delta\psi_\alpha(\mathbf{r})\,. \tag{3.18}$$

The unperturbed part of the wave function satisfies the equation

$$\left[-\frac{\hbar^2\nabla^2}{2m}+V_{\mathrm{eff}}(\mathbf{r})\right]\psi_\alpha^0(\mathbf{r}) = \varepsilon_\alpha^0\psi_\alpha^0(\mathbf{r})\,, \tag{3.19}$$

where

$$V_{\mathrm{eff}}(\mathbf{r}) = \frac{Z_i^{\mathrm{N}}}{|\mathbf{r}|}+\int \mathrm{d}\mathbf{r}\,\frac{\rho_i^0(\mathbf{r}')}{|\mathbf{r}-\mathbf{r}'|}+V_{\mathrm{xc}}(\mathbf{r})+V_{\mathrm{ext}}^0(\mathbf{r},K_0)\,, \tag{3.20}$$

and the change in the wave function, $\delta\psi_\alpha(\mathbf{r})$, is described by the equation

$$\left[-\frac{\hbar^2\nabla^2}{2m}+V_{\mathrm{eff}}(\mathbf{r})-\varepsilon_\alpha\right]\delta\psi_\alpha(\mathbf{r}) = -\left[V_{\mathrm{ext}}(\mathbf{r},K_l)+\frac{\delta V_{\mathrm{eff}}(\mathbf{r})}{\delta\rho(\mathbf{r})}\,\delta\rho(\mathbf{r})\right]\psi_\alpha^0(\mathbf{r})\,. \tag{3.21}$$

In Sternheimer's method, equations (3.19) and (3.21) must be solved self-consistently. For their numerical solution we used an expansion of the wave functions in Chebyshev polynomials. As a result, we found that the change in the wave function depends on the parameter K_0 and is linear in the parameters K_l, so that the change in the charge density has the form

$$\delta\rho^l(\mathbf{r}) = K_l\,\delta\tilde{\rho}_l(\mathbf{r},K_0)\,P_l(\cos\theta)\,. \tag{3.22}$$

In accordance with standard electrodynamics, we can define the multipole moment P_l as

$$P_l = \int \mathrm{d}\mathbf{r}\,r^l P_l(\cos\theta)\,\delta\tilde{\rho}_l(\mathbf{r},K_0)\,, \tag{3.23}$$

and the corresponding polarizability as

$$\alpha_l = \frac{P_l}{K_l} = \int \mathrm{d}\mathbf{r}\,r^l P_l^2(\cos\theta)\,\delta\tilde{\rho}_l(\mathbf{r},K_0)\,. \tag{3.24}$$

This relation makes it possible to replace an external-field parameter by the corresponding multipole moment. The expression for the total energy of an ion in the given external fields has the form

$$E^{\mathrm{ion}}\{\rho(\mathbf{r})\} = \int \mathrm{d}\mathbf{r}\,\frac{Z\rho(\mathbf{r})}{|\mathbf{r}|}+\frac{1}{2}\iint \mathrm{d}\mathbf{r}\,\mathrm{d}\mathbf{r}'\,\frac{\rho(\mathbf{r})\rho(\mathbf{r}')}{|\mathbf{r}-\mathbf{r}'|} + \sum_l \int \mathrm{d}\mathbf{r}\,V_{\mathrm{ext}}(\mathbf{r},K_l)\,\rho(\mathbf{r})+F\{\rho(\mathbf{r})\}\,. \tag{3.25}$$

To find the energy of an ion with a nonequilibrium density distribution for fixed values of the multipole moments, we must, in accordance with the ideas of nonequilibrium thermodynamics, take the following steps. First, from the formula

$$\frac{\delta E^{\mathrm{ion}}}{\delta V_{\mathrm{ext}}(\mathbf{r})} = \rho(\mathbf{r}) \tag{3.26}$$

we must express $V_{\mathrm{ext}}(\mathbf{r})$ in terms of the charge density and plug the resulting expression for $V_{\mathrm{ext}}(\mathbf{r})$ into (3.25). Then we must subtract from (3.25) the energy A related to the work that the external field does in order to produce in the system in question the fixed values of the multipole moments:

$$A = \int \mathrm{d}\mathbf{r}\,V_{\mathrm{ext}}\{\rho(\mathbf{r})\}\,\rho(\mathbf{r})\,. \tag{3.27}$$

All these procedures are trivial in the framework of the density functional method, since the energy is already expressed as a density functional. As a result, for the self-energy of an ion with a nonequilibrium density distribution we have

$$E_{\mathrm{ion}}^{\mathrm{self}} = \int \mathrm{d}\mathbf{r}\,\frac{Z\rho(\mathbf{r})}{|\mathbf{r}|}+\frac{1}{2}\iint \mathrm{d}\mathbf{r}\,\mathrm{d}\mathbf{r}'\,\frac{\rho(\mathbf{r})\,\rho(\mathbf{r}')}{|\mathbf{r}-\mathbf{r}'|}+F\{\rho(\mathbf{r})\}\,. \tag{3.28}$$

The expression for the total energy can now be written as follows:

$$E_{\mathrm{cr}} = E\left\{\sum_i \rho_i(\mathbf{r}-\mathbf{R}_i)\right\}-\sum_i E_{\mathrm{ion}}^{\mathrm{self}}\{\rho_i(\mathbf{r}-\mathbf{R}_i)\} + E^{\mathrm{N}}+\sum_i E_{\mathrm{ion}}^{\mathrm{self}}\{\rho_i(\mathbf{r}-\mathbf{R}_i)\}\,. \tag{3.29}$$

A remark is in order. In Refs [42–44], where attempts were made to generalize the Kim–Gordon model, the first terms on the right-hand side of (3.25) were used in exactly the same form as in Refs [51–53]. This means that the sum of the energies of individual ions, which was subtracted from the total electron energy written as a density functional, was taken in the form (3.28). The differences in opinion began when the question arose as to what precisely should be added to the energy. All the researchers agreed that simply adding the same sum (3.28), which is the most natural approach, would lead to serious difficulties of retaining the necessary accuracy of calculations. The quantity $E_{\mathrm{ion}}^{\mathrm{self}}$ defined by (3.28)

contains very large contributions to the ion energy that are independent of the surroundings of the ion in the crystal. To get rid of these large contributions, we will calculate the change in energy caused by changes in the variational parameters K_l. To this end, we write $E_{\text{ion}}^{\text{self}}$ in the form

$$E_{\text{ion}}^{\text{self}} = E_i^{\text{ion}} - \sum_l \int \mathrm{d}\mathbf{r}\, V_{\text{ext}}(\mathbf{r}, K_l)\, \rho(\mathbf{r}) \tag{3.30}$$

and, correspondingly,

$$\frac{\partial E_{\text{ion}}^{\text{self}}}{\partial K_l} = \frac{\partial E_i^{\text{ion}}}{\partial K_l} - \sum_l \int \mathrm{d}\mathbf{r}\, \frac{\partial V_{\text{ext}}(\mathbf{r}, K_l)}{\partial K_l}\, \rho(\mathbf{r}) - \int \mathrm{d}\mathbf{r}\, V_{\text{ext}}(\mathbf{r}, K_l)\, \frac{\partial \rho(\mathbf{r})}{\partial K_l}\,. \tag{3.31}$$

The minimum condition imposed on the functional E_i^{ion} yields

$$\frac{\partial E_i^{\text{ion}}}{\partial K_l} = \sum_l \int \mathrm{d}\mathbf{r}\, \frac{\partial V_{\text{ext}}(\mathbf{r}, K_l)}{\partial K_l}\, \rho(\mathbf{r}) \tag{3.32}$$

and, finally,

$$\frac{\partial E_{\text{ion}}^{\text{self}}}{\partial K_l} = -\int \mathrm{d}\mathbf{r}\, V_{\text{ext}}(\mathbf{r}, K_l)\, \frac{\partial \rho(\mathbf{r})}{\partial K_l}\,. \tag{3.33}$$

The total change in $E_{\text{ion}}^{\text{self}}$ caused by variations in the parameters is given by the formula

$$\Delta E_{\text{ion}}^{\text{self}} = -\sum_l \int \mathrm{d}K \int \mathrm{d}\mathbf{r}\, V_{\text{ext}}(\mathbf{r}, K_l)\, \frac{\partial \rho(\mathbf{r})}{\partial K_l}\,. \tag{3.34}$$

Bearing in mind the linear relationship (3.24) between the parameters K_l and the multipole moments P_l, we arrive at an expression for the self-energy of the ion with multipole change in its density at $l > 0$ by integrating (3.34) from 0 to K_l:

$$E_{\text{ion}}^{\text{self}} = \frac{\mathbf{P}_l^2}{2\alpha_l}\,. \tag{3.35}$$

This is a well-known formula from classical electrostatics [26]. The reasons why we cannot calculate the energy at $K_0 = 0$ for a monopole distortion of the density have been discussed earlier [see (3.14)]. Hence, to calculate the energy difference that emerges under small distortions we must integrate (3.34) over K_0 in an interval that contains the small region of real variations in K_0. Now we can write the expression for the total energy of the crystal by employing equation (3.29). As in the rigid ion model, we limit ourselves to pair overlaps of ions. Grouping in the first term on the right-hand side of (3.29) the terms with a spherically symmetric charge distribution and multipole moments, we obtain [50, 51, 53]

$$E_{\text{cr}} = \sum_i E_i^{\text{self}}(K_0^i) + \sum_{i,i'} E_{ii'}^{\text{sr}}\big(K_0^i, K_0^{i'}, |\mathbf{R}_i - \mathbf{R}_{i'}|\big) + \frac{1}{2}\sum_{ii'} \frac{Z_i^{\text{ion}} Z_{i'}^{\text{ion}}}{|\mathbf{R}_i - \mathbf{R}_{i'}|} + \sum_l \sum_i \frac{(\mathbf{P}_i^{(l)})^2}{2\alpha_i^{(l)}} + \sum_{l,l'} \sum_{i,i'} \mathbf{P}_i^{(l)} C_{ii'}^{ll'} \mathbf{P}_{i'}^{(l')} + \sum_{l,l'} \sum_{i,i'} \mathbf{P}_i^{(l)} \Phi_{ii'}^{ll'}(K_0^i, K_0^{i'}) \mathbf{P}_{i'}^{(l')}\,. \tag{3.36}$$

Here, the first term is the self-energy of a spherically symmetric ion. The second term is the contribution of the short-range repulsion caused by the overlap of spherically symmetric extended ions. For all practical purposes, this term coincides with the one obtained earlier [see (3.13)] in the rigid ion model, but it contains an additional contribution to self-energy related to changes in the variational parameter K_0. The third term is the standard Coulomb interaction between point ions. The fourth term is the self-energy of point multipole moments ($l = 1$ corresponds to the dipole moment, $l = 2$ to the quadrupole moment). The fifth term represents the Coulomb interaction of point multipoles. Finally, the sixth term describes the short-range interaction between extended multipoles. The matrices $\Phi_{ii'}^{(ll')}$ must be obtained through numerical calculations, whose details are described in Refs [50, 51, 53], so that we will not dwell on them any further.

If we take into account only the dipole distortions of the charge density, the total energy of the crystal becomes

$$E_{\text{cr}} = \sum_i E_i^{\text{self}}(K_0^i) + \sum_{i,i'} E_{ii'}^{\text{sh}}\big(K_0^i, K_0^{i'}, |\mathbf{R}_i - \mathbf{R}_{i'}|\big) + \frac{1}{2}\sum_{ii'} \frac{Z_i^{\text{ion}} Z_{i'}^{\text{ion}}}{|\mathbf{R}_i - \mathbf{R}_{i'}|} + \sum_i \frac{(\mathbf{P}_i^{(1)})^2}{2\alpha_i^{(1)}} + \frac{1}{2}\sum_{\alpha,\beta,i,i'} P_{i,\alpha}^{(1)} C_{ii',\alpha\beta}^{(11)}\big(|\mathbf{R}_i - \mathbf{R}_{i'}|\big) P_{i',\beta}^{(1)} + \frac{1}{2}\sum_{\alpha,\beta,i,i'} P_{i,\alpha}^{(1)} \Phi_{ii',\alpha\beta}^{(11)}\big(K_0^i, K_0^{i'}, |\mathbf{R}_i - \mathbf{R}_{i'}|\big) P_{i',\beta}^{(1)} - \sum_{\alpha,i} P_{i,\alpha}^{(1)} e_i^{\alpha} - \sum_{\alpha,i} P_{i,\alpha}^{(1)} E_i^{\alpha}\,, \tag{3.37}$$

where $\mathbf{P}_i^{(1)}$ is the dipole moment of the ion and $\alpha_i^{(1)}$ is the dipole polarizability. The matrix $C_{ii',\alpha\beta}^{(11)}(|\mathbf{R}|)$ has the form

$$C_{ii',\alpha\beta}^{(11)}(\mathbf{R}) = \frac{\delta_{\alpha\beta}}{R^3} - \frac{R_\alpha R_\beta}{R^5}\,, \qquad \mathbf{R} = \mathbf{R}_i - \mathbf{R}_{i'}\,, \tag{3.38}$$

the matrix $\Phi_{ii'}^{(11)}$ describes the short-range interaction between extended dipoles, and the vector e_i^{α} describes the interaction of dipoles with the electric field induced by the spherically symmetric distribution of the electron density. Formally, the matrices $\mathbf{C}$ and $\mathbf{\Phi}$ and the vector $\mathbf{e}$ can be written as follows:

$$C_{ii'}^{(11)} + \Phi_{ii'}^{(11)} = \frac{\partial^2}{\partial \mathbf{P}_i^{(1)}\, \partial \mathbf{P}_{i'}^{(1)}} \big[E\big\{\rho_i(\mathbf{P}_i^{(1)}, \mathbf{r}) + \rho_{i'}(\mathbf{P}_{i'}^{(1)}, \mathbf{r})\big\} - E_i\big\{\rho_i(\mathbf{P}_i^{(1)}, \mathbf{r})\big\} - E_{i'}\big\{\rho_{i'}(\mathbf{P}_{i'}^{(1)}, \mathbf{r})\big\}\big]\,, \tag{3.39}$$

$$e_i = -\frac{\partial}{\partial \mathbf{P}_i^{(1)}} \big[E\big\{\rho_i(\mathbf{P}_i^{(1)}, \mathbf{r}) + \rho_{i'}(\mathbf{P}_{i'}^{(1)}, \mathbf{r})\big\} - E_i\big\{\rho_i(\mathbf{P}_i^{(1)}, \mathbf{r})\big\}\big]\,. \tag{3.40}$$

The last term on the right-hand side of (3.37) describes the interaction between dipoles and an electric field, which can be an external field or the electric field generated by the displacement of atoms from their equilibrium positions, which is important in describing the lattice dynamics. The quadrupole distortions of the electron density on ions is taken into account in the same manner; for more details about the effect of such distortions on the structural properties and lattice dynamics see the next section of this review.

Here, we use, for the time being, formula (3.37) for the crystal's total energy and calculate the electron contribution

to the dielectric constant ε_∞ of the system; we assume that $\mathbf{E}_i$ is an external electric field and set it equal to a constant: $\mathbf{E}_i = \text{const}$. The condition of minimum energy

$$\frac{\partial E_{\text{cr}}}{\partial \mathbf{P}_i^{(1)}} = 0 \tag{3.41}$$

yields

$$\mathbf{P}_i^{(1)} = \alpha_i^{(1)}\mathbf{E}_i - \alpha_i^{(1)} \sum_{i'} C_{ii'}^{(11)} \mathbf{P}_{i'}^{(1)} - \alpha_i^{(1)} \sum_{i'} \Phi_{ii'}^{(11)} \mathbf{P}_{i'}^{(1)} . \tag{3.42}$$

In deriving (3.42) we set $e_i = 0$, which holds for a crystal with an inversion center.

The last term on the right-hand side of (3.42) can be removed by introducing what is known as nonlocal polarizability:

$$\alpha_{ii'}^{(1)} = (\delta_{ii'} + \alpha_i^{(1)} \Phi_{ii'}^{(11)})^{-1} \alpha_{i'}^{(1)} . \tag{3.43}$$

We represent the position coordinates of ions in the lattice as

$$\mathbf{R}_i = \mathbf{R}_n + \mathbf{s}_i , \tag{3.44}$$

where $\mathbf{R}_n$ is the Bravais lattice vector describing the coordinates of a unit cell, and $\mathbf{s}_i$ specifies the position of an atom in the cell. It has proven convenient to write the interaction matrix for point dipoles in the following form:

$$C_{ii'}^{(11)} = C_{nn'}^{(11)} - \gamma_{ii'} , \tag{3.45}$$

where the matrix $C_{nn'}^{(11)}$ describes the dipole–dipole interaction between cells and does depend on the position of the atom inside the cell. In the case of diatomic crystals of cubic symmetry, the matrix $\gamma_{ii'}$ is identically equal to zero. In crystals with a more complicated structure or of noncubic symmetry, the matrix $\gamma_{ii'}$ is not zero, but it is short-range [56] and decreases with increasing distance faster than $1/|\mathbf{R}_i - \mathbf{R}_{i'}|^5$. In the case of a homogeneous electric field, the polarization of the crystal is also homogeneous:

$$\mathbf{P} = \frac{1}{v} \sum_i \mathbf{P}_i^{(1)} = \frac{1}{v_0} \sum_s \mathbf{P}_s^{(1)} . \tag{3.46}$$

The matrix $C_{nn'}^{(11)}$ exhibits an important property [9, 16, 56]:

$$\sum_{n'} C_{nn',\alpha\beta}^{(11)} = -\frac{4\pi}{3v_0} \delta_{\alpha\beta} . \tag{3.47}$$

If we take (3.45) and (3.46) into account, equation (3.41) becomes

$$\mathbf{P}_i^{(1)} = \sum_{i'} \alpha_{ii'}^{(1)} \mathbf{E} + \frac{4\pi}{3} \sum_{i'} \alpha_{ii'}^{(1)} \mathbf{P} + \sum_{i',i''} \alpha_{ii'}^{(1)} \gamma_{i'i''} \mathbf{P}_{i''}^{(1)} . \tag{3.48}$$

Note that the nonlocal polarizability matrix is, by definition (3.42), short-range. We can solve equation (3.45) and, allowing for the definition of the dielectric constant

$$\varepsilon_\infty = 1 + \frac{4\pi \mathbf{P}}{\mathbf{E}} , \tag{3.49}$$

we finally get

$$\varepsilon_\infty = 1 + \frac{4\pi \alpha_{\text{c}}^{(1)}}{1 - (4\pi/3)\alpha_{\text{c}}^{(1)}} . \tag{3.50}$$

Here, $\alpha_{\text{c}}^{(1)}$ is the unit-cell polarizability:

$$\alpha_{\text{c}}^{(1)} = \frac{1}{v_0} \sum_{s,i,i',i''} (\delta_{si} - \alpha_{si}^{(1)} \gamma_{ii'})^{-1} \alpha_{i'i''}^{(1)} . \tag{3.51}$$

Summation over s in (3.51) is done within a single unit cell, while summation over the other indices is done within the entire crystal.

The first thing that must be said here is that we have arrived at an expression of the Clausius–Mossotti type for the dielectric constant of a crystal. For diatomic crystals, in the approximation of a polarizable point ion, $\gamma_{ii'} = 0$ and $\Phi_{ii'}^{(11)} = 0$, so that the unit-cell polarizability is reduced to the well-known formula

$$\alpha_{\text{c}}^{(1)} = \alpha_1^{(1)} + \alpha_2^{(1)} , \tag{3.52}$$

where $\alpha_1^{(1)}$ and $\alpha_2^{(1)}$ are the polarizabilities of free ions. In the general case of crystals with overlapping extended dipoles and in the presence of a matrix of non-Lorentz local-field factors, $\gamma_{ii'}$, the polarizability of the unit cell cannot be reduced to the sum of free-ion polarizabilities. We can formally define the unit-cell polarizability as the sum of polarizabilities of individual ions:

$$\alpha_{\text{c}}^{(1)} = \frac{1}{v_0} \sum_s \alpha_s^{\text{ion}} , \tag{3.53}$$

where

$$\alpha_s^{\text{ion}} = \sum_{i,i',i''} (\delta_{si} - \alpha_{si}^{(1)} \gamma_{ii'})^{-1} \alpha_{i'i''}^{(1)} . \tag{3.54}$$

In the case of a diatomic crystal this expression becomes

$$\alpha_s^{\text{ion}} = \sum_i \alpha_{si}^{(1)} . \tag{3.55}$$

As shown earlier in Ref. [48], due to the small overlap of extended dipoles in alkali halide crystals we have $\alpha_s^{\text{ion}} \approx \alpha_s^{(1)}$, where $\alpha_s^{(1)}$ is the free-ion polarizability. When we are dealing with alkaline-earth oxides [50], however, α_s^{ion} and $\alpha_s^{(1)}$ differ significantly. In concluding our discussion of the dielectric constant we note that the existence of a Clausius–Mossotti relation for ε_∞ is a direct corollary of the long-range dipole–dipole interaction between unit cells. Using formula (3.36), we can derive an analytical expression for Born's dynamical charge [9], which describes the appearance of polarization in the crystal as the result of displacements of the ion sublattices, displacements that correspond to the transverse polar optical mode when the momentum $\mathbf{q}$ is zero. The change in the polarization has the form

$$\delta\mathbf{P} = \frac{1}{v_0} \sum_s Z^{\text{ion}} \mathbf{u}_s + \sum_s \mathbf{P}_s . \tag{3.56}$$

The change in the electron polarization can be calculated with the help of (3.37), and the result is

$$\delta\mathbf{P} = \frac{1}{v_0} \sum_s Z^{\text{eff}} \mathbf{u}_s , \tag{3.57}$$

where Z^{eff} is the effective Born charge, which, among other things, determines the splitting of frequencies of longitudinal

and transverse modes at $\mathbf{q} = 0$:

$$\omega_{\mathrm{LO}}^2 - \omega_{\mathrm{TO}}^2 = \frac{4\pi (Z^{\mathrm{eff}})^2}{\mu v_0 \varepsilon_\infty} . \tag{3.58}$$

For $\mathbf{P}_s$ we can write the equation

$$\mathbf{P}_s = \alpha_s^{(1)} \mathbf{E}_s - \alpha_s^{(1)} \sum_i C_{si}^{(11)} \mathbf{P}_i^{(1)} - \alpha_s^{(1)} \sum_i \Phi_{si}^{(11)} \mathbf{P}_i^{(1)} + \sum_i m_{si} Z_i^{\mathrm{ion}} \mathbf{u}_i . \tag{3.59}$$

Here, writing the vector $\mathbf{e}_i$ (3.37) for small displacements as

$$\mathbf{e}_i = \sum_{i'} m_{ii'} Z_{i'}^{\mathrm{ion}} \mathbf{u}_{i'} , \tag{3.60}$$

we have introduced the nonlocal ion deformability m_{si}. The electric field at the site s for small ion displacements has the form

$$\mathbf{E}_s = - \sum_i \tilde{C}_{si}^{(11)} Z_i^{\mathrm{ion}} \mathbf{u}_i , \tag{3.61}$$

where

$$\tilde{C}_{si}^{(11)} = C_{si}^{(11)} - \delta_{si} \sum_{i'} C_{ii'}^{(11)} . \tag{3.62}$$

Using expression (3.43) for nonlocal polarizability, we can write (3.59) in the form

$$\mathbf{P}_s = \sum_i \alpha_{si}^{(1)} \mathbf{E}_i - \sum_{i,i'} \alpha_{si}^{(1)} C_{ii'}^{(1)} \mathbf{P}_{i'} - \sum_i \tilde{m}_{si} Z_i^{\mathrm{ion}} \mathbf{u}_i , \tag{3.63}$$

where

$$\tilde{m}_{ii'} = \sum_{i''} \alpha_{ii''}^{(1)} m_{i''i'} . \tag{3.64}$$

Formally, equation (3.63) for $\mathbf{P}_s$ coincides with the expression for this quantity obtained in the most general phenomenological theory of ionic crystals, which allows for nonlocal polarizability and nonlocal deformability of ions [10]. The equation for $\mathbf{P}_s$ can be solved by a method similar to the one used to calculate the dielectric constant. As a result of calculations, we arrive at an expression for the effective Born charges:

$$Z_s^{\mathrm{eff}} = \left(1 - \frac{1}{v_0} \frac{4\pi}{3} \alpha_{\mathrm{c}}^{(1)} \right)^{-1} \xi(s) = \frac{\varepsilon_\infty + 2}{3} \xi(s) , \tag{3.65}$$

where

$$\xi(s) = \sum_{t,i,i'} \left(1 - \frac{1}{v_0} \alpha\gamma \right)_{ts}^{-1} \left(1 - \frac{1}{v_0} \alpha\gamma \right)_{si} (1 - m)_{ii'} Z_{i'}^{\mathrm{ion}} . \tag{3.66}$$

The factor $(\varepsilon_\infty + 2)/3$ in the expression for the effective charge characterizes the well-known [57] increase in the external dipole moment in a polarizable medium. Expressions (3.65) and (3.66) formally coincide with those obtained earlier in Ref. [16] in the model of a polarizable point ion. The difference is that the above formulas incorporate nonlocal polarizabilities. Moreover, expression (3.65) contains an additional factor characterizing ion deformability, leading, as a result, to a decrease in the nominal ion charge Z_i^{ion}.

Expanding expression (3.36) for the total energy of an ionic crystal, an expression that takes into account the monopole, dipole, and quadrupole ion polarizabilities in a power series in small ion displacements from equilibrium positions, we can write the full expression for the dynamical matrix of the crystal, which can be found in Ref. [54]. As noted earlier, formally such expressions coincide with those derived in the most general phenomenological model of deformable and polarizable ions. The above approach differs from the phenomenological one in that all the quantities and matrices are calculated within our variant of the density functional method without any adjustable parameters.

Recently, a method for calculating the properties of ionic crystals closely resembling the above method was used by a group of German researchers from the University of Münster to calculate the dipole polarizability and the lattice dynamics for a number of simple binary compounds [58] and for the insulating phase of the high-T_c superconductor La_2CuO_4 [59]. Falter et al. [58, 59] pointed to two important (from the viewpoint of the researchers) differences in their approach to calculating the properties of ionic crystals compared to our method.

The first difference is that in calculating the properties of an individual ion they use a special atomic program, which removes a defect in the local electron density approximation, a defect associated with the presence in this approximation of a nonphysical interaction of an electron with itself, i.e., self-interaction. Self-interaction effects manifest themselves most vividly in light ions with a small number of electrons and in ions of transition and rare-earth elements due to the strong localization of the wave functions of d- and f-electrons. We fully agree with the need to step outside the local density approximation in calculating such ions (a discussion of the various ways of surpassing the local approximation and references to the literature can be found in Kohn's Nobel lecture [19]). Furthermore, this fact was mentioned in our first publication [48], where we showed that the use of a generalized gradient approximation within the framework of the Becke model leads to a substantial improvement in the accuracy of the calculated values of ε_∞ for oxides of alkaline-earth metals.

The other difference in Refs [58, 59], namely, the choice of an effective ion charge that differs from its nominal value, is not justified in our opinion. The possibility of selecting an effective ion charge has been discussed by Chizmeshya [60] within the framework of a spherical charge density distribution. The effective charge in Ref. [60] was determined from the minimum energy condition and it was found to differ from the nominal ion charge by a negligible quantity.

4. Calculations of the dielectric constant, lattice dynamics, and structural stability of ionic crystals

In this section we study, within the approach discussed in Section 3 or its variations, the results of calculations of structural properties, vibration frequencies of the crystal lattice, and the dielectric constant for several classes of compounds commonly known as ionic crystals. Among ionic crystals, the simplest crystal structure is that of diatomic alkali-halide compounds and oxides of alkaline-earth metals. As noted in Section 3, the method that takes (3.1) as the electron density of the crystal was used by Kim and Gordon [39] to calculate the properties of a number of

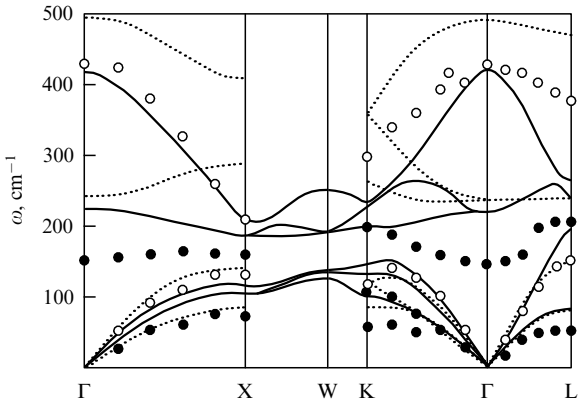

Figure 1. Dispersion curves $\omega(\mathbf{q})$ for the BaO crystal. The solid curves represent the results of calculations done in Ref. [54], the dotted curves represent the results of calculations done in Ref. [61], and the circles represent the experimental data (full and open circles represent transverse and longitudinal branches, respectively) taken from Chang S S et al. *J. Phys. Chem.* **36** 769 (1975).

alkali halide crystals. The results of calculations of the cell parameters and the elastic constants agree rather well with the experimental data. However, as noted earlier, the rigid ion model used in Ref. [39] cannot be applied to oxide compounds. The Kim – Gordon model that allows for the deformability of ions via a Watson sphere whose radius is chosen by the condition that the potential of this sphere be equal to the electrostatic Madelung potential on a given ion (known also as the potential-induced breathing, or PIB, model) [42, 61] provides a satisfactory description of the equilibrium properties (cell parameters and the bulk modulus) of oxides of alkaline-earth metals and a less satisfactory description of the spectrum of lattice vibrations [61]. The discrepancy between the theoretical and experimental values of the vibration frequencies suggests that we must take into account the multipole distortions of the electron density of ions in lattice dynamics calculations. Indeed, the vibrational spectra of diatomic alkali-halide compounds and oxides of alkaline-earth metals calculated in [49, 54] within the same PIB model but allowing for the dipole polarizability of ions agree satisfactorily with the experimental data, as shown by Fig. 1, which depicts, by way of example, the vibrational spectrum of the BaO crystal. However, as shown in Refs [44, 50], the potential of the Watson sphere for an ion in the crystal is not equal to the Madelung potential on the given ion, and this potential should by found from the minimum condition imposed on the total energy of the crystal, as described in Section 3.

To calculate the frequency spectrum of lattice vibrations and the dielectric constant, the expression for the crystal's total energy (3.36) can be expanded in a power series of small ion displacements from the equilibrium positions. This leads to an expression for the dynamical vibration matrix. The dynamical matrix contains contributions from long-range Coulomb interactions (charge – charge, dipole – charge, dipole – dipole, quadrupole – charge, and quadrupole – dipole) and the matrices describing short-range contributions. The Coulomb contributions to the dynamical matrix were calculated by the Ewald method [7], while the short-range contributions were calculated by a technique in which the dependence of the total energy on the distance **R** was approximated with the help of Chebyshev polynomials [50].

We discuss the calculation of the lattice dynamics within the above approach using the example of oxide and halide compounds with the perovskite structure [62] with a general chemical formula ABX_3, where A and B are metal atoms and X is oxygen or halogen. Oxides with the perovskite structure have been studied experimentally and theoretically for more than six decades. The primary reason for the interest in these compounds lies in the fact that many of them are ferroelectrics and antiferroelectrics. In the last twenty years, calculations of the band structure, atomic properties, and the vibrational spectra of the crystal lattice of oxides with the perovskite structure have been carried out by various methods within the density functional theory [the first-principles pseudopotential method, the linear muffin-tin orbital (LMTO) method, the linear augmented plane wave (LAPW) method, and other methods] [23 – 25, 63 – 70]. In particular, as a result of these very successful calculations, new phenomena have been discovered in crystals, namely, ferroelectric instability in $BaTiO_3$ [23, 63, 70], $PbTiO_3$ [68], and $KNbO_3$ [65, 66]; antiferroelectric instability in $PbZrO_3$ [63]; and antiferrodistortion instability in $SrTiO_3$ [69]. A giant LO – TO splitting of polar modes related to the large values of the effective Born charges on ions was obtained. However, as the above reasoning shows, first-principles calculations based on the solution of Kohn – Sham equations [18] are too cumbersome. This factor makes it very difficult to see the real physical reason for one property of the crystal or another, in particular, the reason for ferroelectric instability in oxides with the perovskite structure. At the same time, the lattice dynamics and the dielectric properties of oxides with the perovskite structure have been calculated in the phenomenological models of ionic crystals [16], in which both the crystal properties and the nature of ferroelectric instability are physically transparent, so to say.

In Ref. [62], the equilibrium volumes, the high-frequency dielectric constants, the effective Born charges, and the vibration frequency spectra for a number of oxides with the perovskite structure have been calculated within the described approach. Some results of these calculations and the results of the above-mentioned *ab initio* calculations (given for the sake of comparison) are listed in Tables 1 and 2 and are illustrated by Fig. 2. Both the tables and the figure show that the results of the given calculation agree quite well with the results of the other calculations, although our values of the cell parameters, the dielectric constant, and the effective Born charges are lower by several percent. As noted in Ref. [48], the value of the equilibrium volume is understated because of a defect in the model of a homogeneous electron gas for ions with high polarizability and because the Thomas – Fermi approximation for the total crystal energy is used. The lattice vibration frequencies (see Table 2 and Fig. 2) are in better agreement with the frequencies calculated by other methods. As for the dielectric constant and the effective Born charges, their values are understated because their calculation was done with the theoretical values of the lattice parameters. When these values are raised to the experimental values, both ε_∞ and the Born charges grow to values that are much closer to the results of other researchers. In Table 2, the numbers with an 'i' indicate imaginary frequencies, which correspond to unstable phonon modes.

Here, it is important to note that a comparison of the vibration frequencies in the model of unpolarizable ions (the PIB model) and the same frequencies in the model that allows for dipole and quadrupole polarizabilities of ions clearly

Table 1. Calculated lattice parameters, dielectric constants, quadrupole moments, and effective Born charges for ABO_3 perovskites compared with results of other calculations.

Crystal	a_0, Å		ε_∞		q_{zz}	$Z^*(A)$	
	Present calculation	Other calculations	Present calculation	Other calculations	Present calculation	Present calculation	Other calculations
$BaTiO_3$	3.86	4.00 [b]	5.25	6.75 [b]	1.07	2.90	2.75 [a] 2.74 [b]
$SrTiO_3$	3.78	3.92 [f]	4.26	6.63 [f]	0.93	2.69	2.55 [a] 2.55 [f]
$PbTiO_3$	3.84	3.97 [d]	4.90	8.24 [d]	0.91	2.75	3.90 [a] 3.87 [d]
$CaTiO_3$	3.73		4.52		0.94	2.76	2.58 [a]
$PbZrO_3$	4.02	4.12 [b]	4.56	6.97 [b]	1.00	2.75	3.92 [a]
$BaZrO_3$	4.05		4.56		1.09	2.83	2.73 [a]
$NaNbO_3$	3.76		3.89		1.75	1.28	1.13 [a]
$KNbO_3$	3.74	4.00 [e]	4.01	4.7 [c]	1.73	1.28	1.14 [a]

Crystal	$Z^*(B)$		$Z^*_\perp(O)$		$Z^*_\parallel(O)$	
	Present calculation	Other calculations	Present calculation	Other calculations	Present calculation	Other calculations
$BaTiO_3$	6.31	7.16 [a] 7.32 [b]	−1.59	−2.14 [b] −2.11 [a]	−6.02	−5.78 [b] −5.69 [a]
$SrTiO_3$	5.97	7.12 [a] 7.56 [f]	−1.66	−2.12 [f] −2.00 [a]	−5.32	−5.65 [a] −5.92 [f]
$PbTiO_3$	5.87	7.06 [a] 7.04 [d]	−1.65	−2.56 [a] −2.57 [d]	−5.30	−5.83 [a] −5.76 [d]
$CaTiO_3$	6.29	7.08 [a]	−1.77	−2.00 [a]	−5.51	−5.65 [a]
$PbZrO_3$	5.64	5.85 [a] 5.89 [b]	−1.92	−2.48 [a] −2.50 [b]	−4.56	−4.81 [a] −4.82 [b]
$BaZrO_3$	5.75	6.03 [a]	−1.88	−2.01 [a]	−4.81	−4.74 [a]
$NaNbO_3$	7.52	9.11 [a]	−1.27	−1.61 [a]	−6.25	−7.01 [a]
$KNbO_3$	7.10	9.23 [a]	−1.35	−1.70 [a]	−5.70	−7.01 [a]

a — The pseudopotential and 'frozen' phonon methods [Zhong W, King-Smith R D, Vanderbilt D *Phys. Rev. Lett.* **72** 3618 (1994)]
b — The pseudopotential and linear response methods [Ghosez Ph et al. *Phys. Rev. B* **60** 836 (1999)]
c — The Hartree–Fock approximation [Fu L et al. *Phys. Rev. B* **57** 6967 (1998)]
d — LAPW [Yu R, Wang C-Z, Krakauer H *Ferroelectrics* **164** 161 (1995)]
e — LMTO and the 'frozen' phonon method [Postnikov A V, Neumann T, Borstel G *Ferroelectrics* **164** 101 (1995)]
f — LAPW [Lasota C et al. *Ferroelectrics* **194** 109 (1997)]

shows that, in full agreement with the results of phenomenological models of ionic crystals, the ferroelectric instability in oxides with the perovskite structure is determined primarily by the strong long-range dipole–dipole forces.

Our approach to calculations of the dielectric constant, the effective Born charges, and phonon spectrum in perovskite crystals makes it possible to easily determine the reason for the various features in the behavior of these quantities, also recorded in other theoretical studies [63–68]. First, we are speaking of the fact that a characteristic feature of perovskites is their large effective Born charges, which are much larger than the nominal ion charges. What is important is that there is a strong correlation between the effective charges on different ions. Note that in a cubic structure, for which our calculations were done, the metal atoms A and B are positioned at the centers of cubic symmetry, and the tensors of their effective charges are isotropic. On the other hand, the oxygen (or halogen) ion lies in the cube's plane and has two nonequivalent directions, one perpendicular to the $B-O$ axis and the other parallel to this axis, and, respectively, two values of the effective charge, $Z^*_\perp(O)$ and $Z^*_\parallel(O)$. Table 1 shows that for all the compounds listed the effective charges

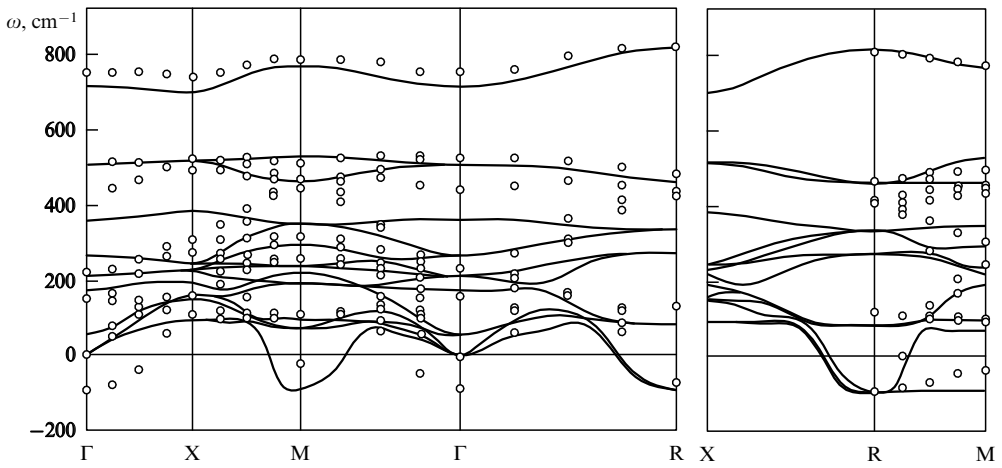

Figure 2. Dispersion curves $\omega(\mathbf{q})$ for the $SrTiO_3$ crystal. The solid curves represent the results of calculations done in Ref. [62] and the open circles represent the results of calculations done in Ref. [66].

Table 2. Calculated optical phonon frequencies (in cm^{-1}) for ABO_3 perovskites compared with results of other calculations.

Crystal		TO1		TO2		TO3		T_{2u}		LO1		LO2		LO3	
		Present calculation	Other calculations	Present calculation	Other calculations	Present calculation	Other calculations	Present calculation	Other calculations	Present calculation	Other calculations	Present calculation	Other calculations	Present calculation	Other calculations
$BaTiO_3$	PIB	156		438		620		302		196		620		833	
		47i	178i [a] 210i [b]	233	177 [a] 170 [b]	418	468 [a] 450 [b]	192	290 [b]	155	173 [a] 170 [b]	322	453 [a] 450 [b]	637	738 [a] 620 [b]
$SrTiO_3$	PIB	147		455		656		288		209		652		858	
		53	41i [a] 100i [f]	265	165 [a] 151 [f]	505	546 [a] 522 [f]	208	219 [f]	171	158 [a] 146 [f]	358	454 [a] 439 [f]	713	829 [a] 751 [f]
$PbTiO_3$	PIB	142		438		628		311		181		628		833	
		81i	144i [a] 180i [b]	238	121 [a] 80 [b]	422	497 [a] 450 [b]	186	230 [b]	136	104 [a] 70 [b]	323	410 [a] 415 [b]	615	673 [a] 610 [b]
$CaTiO_3$	PIB	121		471		699		250		248		676		896	
		86i	153i [a]	287	188 [a]	574	610 [a]	182		189	133 [a]	367	427 [a]	779	866 [a]
$PbZrO_3$	PIB	101		367		627		240		140		593		740	
		91i	131i [a] 140i [b]	217	63 [a] 170 [b]	485	586 [a] 600 [b]	151	30 [b]	101	90 [a]	283	310 [a]	611	720 [b]
$BaZrO_3$	PIB	100		360		611		230		147		580		729	
		64i	95 [a]	227	193 [a]	484	514 [a]	163		117		294		620	
$NaNbO_3$	PIB	165		456		806		298		210		722		931	
		73	152i [a]	249	115 [a]	634	556 [a]	166		170	101 [a]	319	379 [a]	883	928 [a]
$KNbO_3$	PIB	208		527		777		341		226		727		997	
		61	143i [c] 137i [d]	259	188 [c] 171 [d]	623	506 [c] 482 [d]	147		197	183 [c] 166 [d]	312	407 [c] 404 [d]	861	899 [c] 743 [d]

a — The pseudopotential and 'frozen' phonon methods [Zhong W, King-Smith R D, Vanderbilt D *Phys. Rev. Lett.* **72** 3618 (1994)]
b — The pseudopotential and linear response methods [Ghosez Ph et al. *Phys. Rev. B* **60** 836 (1999)]
c — The Hartree – Fock approximation [Fu L et al. *Phys. Rev. B* **57** 6967 (1998)]
d — LAPW [Yu R, Wang C-Z, Krakauer H *Ferroelectrics* **164** 161 (1995)]
e — LMTO and the 'frozen' phonon method [Postnikov A V, Neumann T, Borstel G *Ferroelectrics* **164** 101 (1995)]
f — LAPW [Lasota C et al. *Ferroelectrics* **194** 109 (1997)]

of the B ion and $Z^*_{\parallel}(O)$ are exceptionally large, while the charges of ion A and $Z^*_{\perp}(O)$ are very close to their nominal values. The $PbTiO_3$ compound demonstrates a certain correlation in the increase in the effective charges on Pb and $Z^*_{\perp}(O)$, too.

Several different explanations of the nature of these correlations in the behavior of effective charges have been proposed (see Refs [63, 70] and references therein). Among these was the assumed possibility of the dynamical flow of charge from the B ion to oxygen during their motion toward each other in an optically active mode. Another speculation concerned the possibility of strong polarization of the $B-O$ bond caused by hybridization of the 2p-state of the oxygen ion and d-orbitals of the B ion. However, all this is mere words used to explain the meaning of the actually calculated values, i.e., the charges of the B ion and $Z^*_{\parallel}(O)$. No calculations of charge flow or bond polarization were done in the above-mentioned works. On the other hand, the results of our calculations point to the real reason for such correlations, which, incidentally, has been known for a long time in the classical physics of ionic crystals [16]. This is nothing more than non-Lorentz local-field corrections described by the matrix $\gamma_{ii'}$ introduced in Section 3. The fact that such corrections exist leads primarily to strong anisotropy in the local field on the oxygen ion. The field in the direction of the B ion is almost ten times stronger than that in the perpendicular direction. This, in turn, leads to strong anisotropy in the polarization of the oxygen ion in the crystal and, according to formula (3.66) for the effective charge, to an increase in the charge on B and $Z^*_{\parallel}(O)$. Note that the matrix element $\gamma_{ii'}$ with the index i corresponding to the B ion and the index i' to the oxygen ion is most important for this phenomenon and $\gamma_{BO} \approx 30$, which is almost ten times larger than the local-field coefficient in binary crystals, where it is equal to $4\pi/3$. The very existence of non-Lorentz corrections and their numerical values are fully determined by the crystal structure of perovskites.

The calculations done in Ref. [52] for the $BaTiO_3$ compound have shown that in a distorted ferroelectric phase the values of the displacements of ions from their equilibrium positions in the cubic phase are in good agreement with the experimental data only if we allow for both dipole and quadrupole distortions in the electron density of the oxygen ions. Allowance for only dipole distortions overstates the value of ion displacements by a factor of almost two and overstates the decrease in the total energy in the ferroelectric phase by a factor of almost ten, as shown in Fig. 3.

In addition to the crystal lattice being ferroelectrically unstable, many oxides with the perovskite structure exhibited other unstable modes in the calculated vibrational spectra. The eigenvectors of these modes correspond to a 'rotation' of the BO_6 octahedron, which is in good agreement with the results of other calculations and with the experimental data. As for the instability of crystals with the perovskite structure with respect to vibrational modes that belong to the boundary points of the Brillouin zone, dipole interactions do not play an important role, and appropriate soft vibrational modes appear even if we allow only for deformation distortions in the electron density of the ions (the PIB model). For instance, in Ref. [71] the PIB model was used to study two types of lattice instability of the $BaBiO_3$ crystal with the perovskite structure. The first type of instability is related to the 'rotation' of the BiO_6 octahedron with respect to the crystallographic axes [110] and [111]. The second type is related to

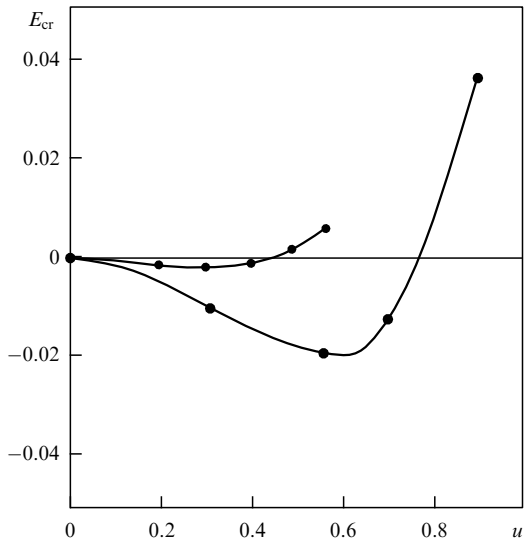

Figure 3. The energy of the $BaTiO_3$ crystal as a function of the displacement amplitude of ions in the ferroelectric phase (the energy is measured from the value of E_{cr} in the cubic phase). The large and small circles correspond to the results of calculations without allowing for quadrupole distortions of the electron density of the oxygen ion and allowing for such distortions, respectively.

what is known as the breathing mode of BiO_6 octahedrons. A characteristic feature of this mode is that there is compression or expansion of oxygen octahedrons (O_6) in relation to the bismuth ion. Usually, this instability in $BaBiO_3$ was associated with the presence in this compound of bismuth ions with different valences, Bi^{3+} and Bi^{5+}, since Bi^{4+} was assumed to be unstable. Accordingly, because of the Coulomb interaction the oxygen octahedron surrounding the Bi^{5+} ion is compressed while the one surrounding the Bi^{3+} ion expands. The structural transition proper is caused by the ordering of Bi^{5+} and Bi^{3+} ions.

Our investigation showed that the nature of the 'breathing' instability in $BaBiO_3$ is much more complicated. First, we did not detect any dynamical instability in the Bi^{4+} ion by itself. Second, the 'breathing' mode of vibrations in itself is not dynamically unstable. Instability emerges when we take into account the combined action of the breathing mode and the charge transfer from one bismuth ion to another, so that $Bi^{4+\delta}$ and $Bi^{4-\delta}$ ions are created. What is important is that the size of the charge transfer, δ, is much smaller than unity. Our analysis of the charge instability of Bi^{4+} ions has shown that, generally speaking, what is known as intermediate valence (i.e., the existence in a crystal of ions of the same element with different valences, which differ by an integer number of electrons) requires further detailed investigation.

In halogen compounds with the perovskite structure, ABX_3, where A is an alkali metal, B a bivalent metal, and X is either F, Cl, or Br, the instability of the crystal lattice is usually related not to polar modes but to vibrational modes belonging to the boundary points of the Brillouin zone. In a series of investigations, Boyer and coworkers [72, 73] used the rigid ion model to calculate the lattice vibration frequencies for a number of halogen compounds. In all the studies of the compounds (more than 60 compounds), the calculated vibrational spectra contain imaginary frequencies, which is an indication of the structural instability of the cubic phase in these crystals. In almost all the compounds (except $AMgF_3$), the spectrum contains a branch of imaginary frequencies

between the points R and M of the Brillouin zone, and in most of these compounds the presence of unstable modes at point X and the vicinity of this point was demonstrated. In some crystals (say, in $NaCaBr_3$, $LiBeF_3$, etc.), the calculated vibrational spectra also exhibited unstable polar modes. The results of the calculations done in the rigid ion model on the whole are in good agreement with the results of experiments, in which the structural phase transitions related to the instability of the vibrational modes belonging to the boundary points of the Brillouin zone (R, M, and X) are observed for practically all halogen compounds with a perovskite structure, while, apparently, ferroelectric phase transitions in these substances have not been detected in experiments.

A calculation of the lattice vibration spectrum by the method discussed in Section 3 for BF_3 crystals, where B is a trivalent metal, crystals that also belong to the perovskite family but have a structure of the ReO_3 type in which the metal positions in the cubic-octahedral surroundings are vacant, was carried out in Refs [74, 75]. The researchers found that under normal pressure the vibration frequency spectrum of the lattice contains no soft modes, i.e., the cubic structure of these compounds remains stable down to $T = 0$. Experiments revealed in AlF_3, GaF_3, and InF_3 crystals a structural phase transition from the cubic phase to the rhombohedral phase, related to the condensation of the threefold degenerate mode R_{25} belonging to the boundary point (111) of the Brillouin zone. In Ref. [74] it was assumed that the structural instability in these compounds is related to defects in the structure, where some of the metal ions occupy cubic-octahedral positions vacant in an ideal structure. Such an assumption is justified to a certain degree by the experimental observation [75] that the isomorphic compound ScF_3 under normal pressure exhibits no structural phase transitions down to liquid-helium temperatures. However, in the calculated lattice-vibrations spectrum of all AF_3 crystals there is a nearly dispersionless vibrational branch between the points M and R of the Brillouin zone with an anomalously low ($\sim 50\ cm^{-1}$) energy value. Figure 4 gives an example of a calculated spectrum of a ScF_3 crystal at $p \approx 0$ and $p = 6$ GPa. The vibration frequencies on the M–R branch of the spectrum decrease when hydrostatic pressure is applied to the crystal, and at a certain value of pressure the cubic phase of the ScF_3 crystal becomes unstable. Indeed, in their experimental study of the vibration frequencies of the ScF_3 crystal by the Raman light scattering method, Aleksandrov et al. [75] discovered a structural phase transition induced by the hydrostatic pressure. Under normal pressure, due to the cubic symmetry of the crystal, there are no Raman-active frequencies (Fig. 5), while under pressures higher than 0.7 GPa the appropriate spectral lines appear. The calculated frequencies of lattice vibrations at $q = 0$ in the expected distorted rhombohedral phase with $R\bar{3}c$ symmetry and with two molecules per unit cell are in satisfactory agreement with the measured values, as Table 3 shows.

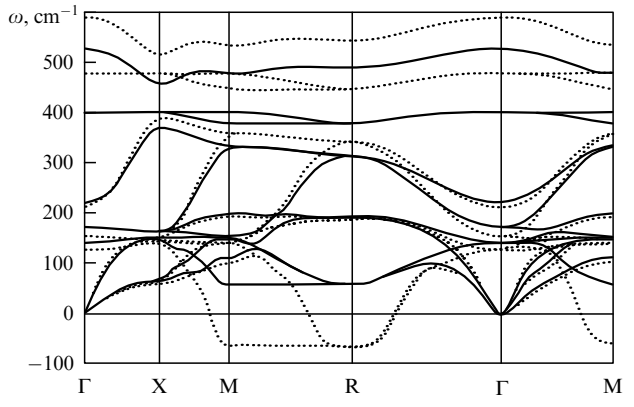

Figure 4. Calculated dispersion curves $\omega(\mathbf{q})$ for the ScF_3 crystal [75]. The solid curves represent the results of calculations under normal pressure and the dotted curves represent the results of calculations at $p = 6$ GPa.

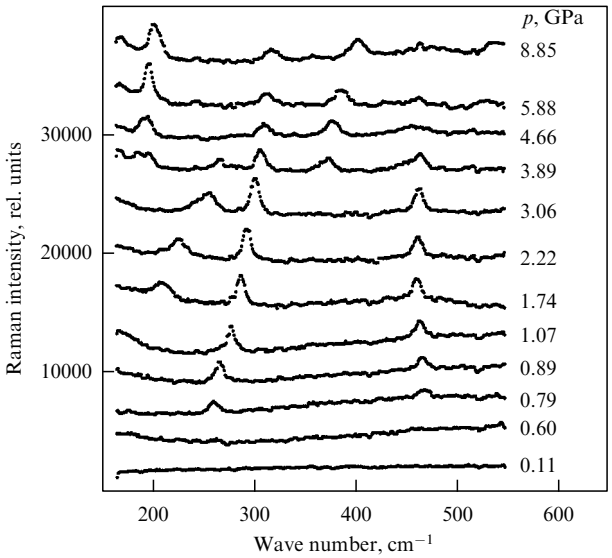

Figure 5. Experimental spectra of Raman scattering in ScF_3 measured in a pressure interval from 0.11 to 8.85 GPa.

Table 3. Calculated vibration frequencies in the rhombohedral phase of ScF_3. The numbers in parentheses are the experimentally measured frequency values.

Rhombohedral ScF_3	
Vibration symmetry	Frequency, cm^{-1}
A_{2u}	557
E_u	442
A_{2u}	210
E_u	164
A_{1u}	148
E_u	132
A_{2g}	513
A_{1u}	327
E_u	330
E_g	412 (465)
A_{2g}	190
E_g	198 (260)
A_{1g}	79 (180)
E_g	34

Allowance for dipole and quadrupole distortions of the electron density of ions is necessary not only in calculations of the vibration spectra of crystals but also in calculations of the structural properties. In particular, in triatomic compounds MX_2, where M is a bivalent metal and X a halogen, and dioxides of tetravalent metals (TiO_2, ZrO_2, etc.), dipole and quadrupole distortions of the electron shells of the ions play the leading role, as shown by Wilson et al. [76, 77], in stabilizing the ground state of one structure or another among several polytypes with close energy values. For instance, in the case of the ZrO_2 crystal, Zhong et al. [63] showed that the monoclinic structure observed in experiments

becomes energy-preferable only if one allows for the polarization energy, which is related to both dipole and quadrupole distortions of the ion electron density, while in the PIB model in ZrO_2 under normal pressures the energy-preferable structure is the cubic structure of the fluorite type [78]. In their calculations of the energies of the different structures, Wilson et al. [76, 77] used the semiempirical model of an ionic crystal with adjustable parameters, whose number becomes large when one allows for the quadrupole distortions of the ion electron densities.

Since our approach to calculating the properties of ionic crystals is not empirical, we discuss in greater detail the effect of the polarization energy on the stability of one structural polytype or another using the example of the ABX_3 compound (A and B are metals and X is oxygen or a halogen). Most oxide compounds belonging to this group, with a small exception ($LiNbO_3$, $LiTaO_3$, $MgTiO_3$, $FeTiO_3$, and a few others) have the perovskite structure. In this structure the cubic phase is usually unstable with respect to one lattice vibration mode or another. Below we discuss such instability in ABO_3 compounds.

The chemical compounds ABX_3, where X is a halogen, may crystallize in various polytypes, which differ in the packing of the BX_6 octahedrons in the structure. The polytypes of these compounds that are encountered most often are the perovskite structure (c-packing), where the BX_6 octahedrons touch each other at the vertices; the two-layer hexagonal structure (h-packing), in which the BX_6 octahedrons are connected to each other by their faces; and the six-layer hexagonal structure (hcc-packing). This third type of packing is a combination of the first two, the c- and h-packings (Fig. 6). Stabilization of one or another of these structures by substituting halogen ions has recently been studied in Ref. [79] for the case of $RbMnX_3$ compounds (X — F, Cl, and Br). The researchers used the method of calculating the structural and dynamical properties of ionic crystals described in Section 3. The energies of the three structures for $RbMnX_3$ were calculated by formula (3.6), and the values of the dipole and quadrupole moments on the ions were found from the minimum condition imposed on the total energy of the crystal:

$$\frac{\partial E^{\mathrm{cr}}}{\partial \mathbf{d}_{\mathrm{ion}}} = 0\,, \qquad \frac{\partial E^{\mathrm{cr}}}{\partial \mathbf{Q}_{\mathrm{ion}}} = 0\,. \tag{4.1}$$

From the viewpoint of the rigid ion model, the formation of hexagonal structures in ABX_3 compounds is not energy-preferable, since in packings in which the BX_6 octahedrons are connected to each other by their faces the B ions are too close to each other, which leads to a loss in Madelung energy compared to that of a perovskite structure. In this case, the short-range spherically symmetric ion–ion interactions remain practically the same. Hexagonal structures can be stabilized only by the polarization energy, which emerges because of the appearance of induced dipole and quadrupole moments on the ions in such structures. What is important here is the competition between the long-range Coulomb interactions between point multipoles and short-range interactions between extended multipoles. In the particular case of ideal structures, the following relations between the unit-cell parameters of the structures in question are valid:

$$\text{c-packing:} \qquad a_{\mathrm{c}} = b_{\mathrm{c}} = c_{\mathrm{c}} = a_0\sqrt{2}\,;$$

$$\text{h-packing:} \qquad a_{\mathrm{h}} = b_{\mathrm{h}} = 2a_0\,, \quad c_{\mathrm{h}} = 2a_0\,\frac{\sqrt{6}}{3}\,;$$

$$\text{hcc-packing:} \qquad a_{\mathrm{h}} = b_{\mathrm{h}} = 2a_0\,, \quad c_{\mathrm{h}} = 2a_0\sqrt{6}\,;$$

and the BX_6 octahedrons are regular. For such structures, allowance only for the long-range Coulomb interactions between point multipoles in the total energy of the crystal leads to a situation in which for all ABX_3 compounds, including oxides, the two-layer hexagonal packing proves to be energy-preferable compared to the perovskite structure and the six-layer hexagonal packing. If we fully take into account the dipole–dipole interactions in the case of ideal structures, we find that the perovskite structure is energy-preferable for all the compounds examined in Ref. [79], although the difference in the total energies of the perovskite structure and the hexagonal structures decreases substantially as the dipole polarizability of the X ion increases (Table 4).

When the ions in the hexagonal structures are relaxed to their equilibrium positions (the X ion in the h-packing has one free coordinate, while in the hcc-packing the ions have five free coordinates) and the deformation, dipole, and quadrupole distortions of the ion electron density are taken into account, the different contributions to the total energy of the crystal are redistributed. The energies of the structures in question with highly polarizable ions (Cl^- and Br^-) become closer, and stabilization of one structure or another is determined by the fine balance between the competing contributions. As a result, it was found (see Ref. [79]) that, in agreement with the experimental data, the stable structure in the $RbMnF_3$ crystal at normal pressures is that of the perovskite type, and it remains stable when hydrostatic pressure is applied. On the other hand, in $RbMnCl_3$ and $RbMnBr_3$ crystals the structure with six-layer hexagonal packing proves to be the energy-preferable one, and in $RbMnCl_3$ this structure is stabilized by quadrupole–quadrupole interactions (see Table 4). On uniform compression, the $RbMnCl_3$ crystal transforms into a perovskite structure at pressures higher than 11 kbar, which agrees very well with the experimental value of this transition, 7 kbar [80].

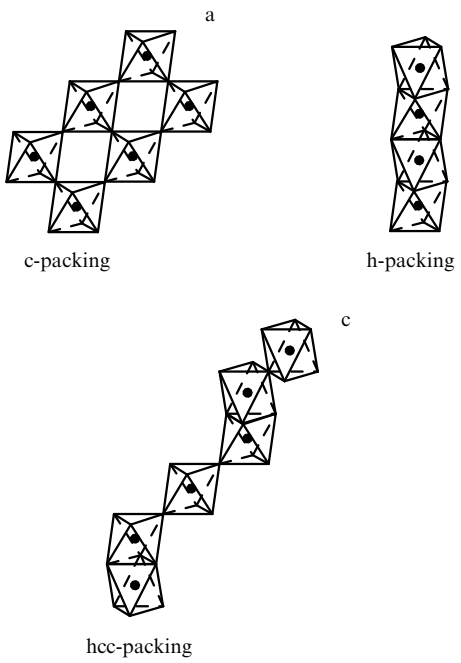

Figure 6. Arrangement of octahedrons in different polytypes of ABX_3.

Table 4. Calculated values (per molecule) of the total energies $E_{\rm tot} = E - E_{\rm self}$ and separate contributions for ideal (I) and relaxed (R) structures.

		$RbMnF_3$ $a_0 = 3.11$ Å			$RbMnCl_3$ $a_0 = 3.63$ Å			$RbMnBr_3$ $a_0 = 3.85$ Å		
		c	h	hcc	c	h	hcc	c	h	hcc
$E^{\rm c}$	I	−40.5623	−37.6163	−39.6310	−34.6722	−32.1426	−33.8919	−32.6861	−30.3322	−32.0129
	R	−40.5623	−39.1902	−40.3444	−34.6722	−32.6301	−33.8317	−32.6861	−29.0245	−31.3275
$E^{\rm s}$	I	3.7548	3.8042	3.7675	2.9107	2.8909	2.8898	2.4462	2.4549	2.4604
	R	3.7548	5.0400	3.9007	2.9107	3.1097	2.8239	2.4462	1.9673	2.4971
$E^{\rm c}_{\rm d-d}$	I	0.0	−2.4809	−0.7853	0.0	−4.0991	−1.3888	0.0	−4.2000	−1.4459
	R	0.0	−2.4313	−0.2443	0.0	−4.1234	−0.8318	0.0	−4.4966	−1.3753
$\tilde{E}$	I	−36.8075	−36.2930	−36.6488	−31.7615	−33.3508	−32.3969	−30.2399	−32.0773	−30.9984
$E^{\rm s}_{\rm d-d}$	I	0.0	1.8489	0.6014	0.0	2.9942	1.0591	0.0	3.0232	1.0873
	R	0.0	2.0824	0.1405	0.0	2.8193	0.1261	0.0	1.8115	−0.1070
$E^{\rm c}_{\rm q-q}$	I	−0.2286	−0.1249	−0.1963	−0.6357	−0.2520	−0.5269	−0.7159	−0.2804	−0.5950
	R	−0.2286	−0.1247	−0.2044	−0.6357	−0.1133	−0.4500	−0.7159	−0.03979	−0.4177
$E^{\rm s}_{\rm q-q}$	I	0.2146	0.1049	0.1803	0.6341	0.2409	0.5225	0.6952	0.2747	0.5850
	R	0.2146	0.1167	0.1870	0.6341	0.0778	0.4072	0.6952	−0.2429	0.2511
$E^{\rm c}_{\rm d-q}$	I	0.0	−0.0697	−0.0211	0.0	−0.1791	−0.1318	0.0	−0.2020	−0.1706
	R	0.0	−0.0812	−0.0095	0.0	−0.1207	−0.0850	0.0	−0.1175	−0.1515
$E^{\rm s}_{\rm d-q}$	I	0.0	0.0568	0.0185	0.0	0.1547	0.1247	0.0	0.1865	0.1692
	R	0.0	0.0748	0.0073	0.0	0.1046	0.0563	0.0	0.0061	0.0591
$E_{\rm tot}$	I	−36.8215	−34.4770	−36.0660	−31.7631	−30.3921	−31.3433	−30.2606	−29.0753	−29.9197
	R	−36.8215	−34.5136	−36.5671	−31.7631	−30.8761	−31.7850	−30.2606	−30.1364	−30.5716

Note. $E^{\rm c}$ is the Madelung energy. $E^{\rm s}$ is the energy of short-range spherically symmetric ion – ion interactions.
$E^{\rm c}_{\rm d-d}$, $E^{\rm c}_{\rm q-q}$, and $E^{\rm c}_{\rm d-q}$ are the energies of long-range dipole – dipole, quadrupole – quadrupole, and dipole – quadrupole interactions.
$E^{\rm s}_{\rm d-d}$, $E^{\rm s}_{\rm q-q}$, and $E^{\rm s}_{\rm d-q}$ are the energies of the short-range respective interactions.
$\tilde{E} = E^{\rm c} + E^{\rm s} + E^{\rm c}_{\rm d-d}$.

5. The use of the polarizable ion model in calculations of structural phase transitions

Calculations of the equilibrium properties, the dielectric constant, the dynamical Born charges, and the vibration-frequency spectrum of the crystal lattice of ionic crystals that use the formulas in Section 2 are done for zero temperature $T = 0$ K. Structural phase transitions, including ferroelectric and antiferroelectric ones, emerge under temperature variations, and many physical properties of ionic crystals are strongly temperature-dependent in the vicinity of the phase transitions.

One approach in calculating the properties of ionic crystals at finite temperatures, including the study of structural transitions, is to use the molecular dynamics and Monte Carlo methods. For instance, Gong and Cohen [81] used the molecular dynamics simulation to study the temperature behavior of a finite $PbTiO_3$ cluster. The researchers applied the PIB+ model (as named by them), in which, as in the PIB model, the dipole polarizability of the ions is ignored, They did, however, introduce additional corrections to the pair interaction, which were determined by comparing the total energy of the crystal calculated in the PIB model and that calculated by the LAPW method. According to Gong and Cohen [81], by introducing these corrections they implicitly allowed for the polarizability of ions and the covalence. As a results of studies of $PbTiO_3$ clusters consisting of 1295 and 1315 particles by the molecular dynamics simulation, the researchers found that in the free state, in accordance with the experiment, small $PbTiO_3$ clusters do not transform into the ferroelectric state and that exclusion of the depolarizing field leads to the instability of the ferroelectric state of the cluster, as opposed to the results of experimental studies.

Edwardson and Hardy [82] also applied the molecular dynamics simulation to study structural transitions in Rb_2ZnCl_4. The short-range ion – ion forces were calculated within the Kim – Gordon model [39]. The researchers found that to describe the structural properties of Rb_2ZnCl_4 correctly requires incorporating in the calculations the dipole moments on the ions. The dipole moments were calculated phenomenologically in the shell model, and their values were determined rather by fitting than by using variational techniques with energy minimization.

An important drawback to employing the direct (i.e., with the use of the complete many-body Hamiltonian) molecular dynamics and Monte Carlo methods is that the calculations done by these methods, especially those involving large systems, are extremely cumbersome. A more productive and very successful approach to calculating the temperatures of phase transitions and the thermodynamic properties of crystals near the transition point is the one that uses the effective Hamiltonian [83 – 86]. The essence of the method is that only the important degrees of freedom are used in

calculating the thermodynamic properties of the crystal, and these important degrees of freedom are the coordinates of the local modes that belong to the soft modes of the vibrations of the crystal lattice. Thus, only a small fraction of the total number of degrees of freedom in the total Hamiltonian are used in calculating the free energy. Here, the parameters of the effective Hamiltonian are determined through calculations of the total energy of the crystal, the elastic constants, and the vibrational spectrum of the crystal lattice. The effective Hamiltonian method was used to calculate the temperatures of the phase transitions and the behavior of the thermodynamic properties near the transition point for several oxides with the perovskite structure that undergo ferroelectric ($PbTiO_3$ [83] and $BaTiO_3$ [85]) and structural ($SrTiO_3$ [86]) phase transitions. Rabe and Waghmare [83], Rabe and Joannopoulos [84], and Vanderbilt and Zhong [86] used the density functional method combined with the pseudopotential approach to calculate the total energy and vibration frequencies of the lattice. The same method was used by Rabe and Joannopoulos [84] to calculate the properties of the ferroelectric compound GeTe.

In all this research a number of inaccuracies were admitted into the process of building the effective Hamiltonian needed to describe the thermodynamics of the ferroelectric substances. First, the Hamiltonian must include the long-range dipole–dipole interaction, which, as is well-known, is the cause of ferroelectric transitions in perovskites. In Refs [83, 86], the contribution of the dipole–dipole interaction was presented in a form obtained by Mahan [57] for the interaction of two external dipoles in a crystal with point polarizable ions. The contribution of this interaction to the lattice energy has the form [85]

$$E^{\mathrm{dip}}\{\mathbf{u}\} = \frac{Z_{\mathrm{eff}}^2}{\varepsilon_\infty} \sum_{i<j} \frac{\mathbf{u}_i \cdot \mathbf{u}_j - 3(\mathbf{R}_{ij} \cdot \mathbf{u}_i)(\mathbf{R}_{ij} \cdot \mathbf{u}_j)}{R_{ij}^3} \,. \tag{5.1}$$

Here, $\mathbf{u}_i$ is the amplitude of the optical vibrational mode in the ith cell, $\mathbf{R}_{ij}$ is the equilibrium ion–ion separation, and Z_{eff} is the effective charge of the vibrational mode. Clearly (see Ref. [87]), the contribution of $E^{\mathrm{dip}}\{\mathbf{u}\}$ to the dynamical vibration matrix as the phonon momentum $q \to 0$ can be written as follows:

$$\Phi_{ij}(q \to 0) = \frac{4\pi Z_{\mathrm{eff}}^2}{v_0} \left[\frac{\mathbf{q}_i \mathbf{q}_j}{q^2 \varepsilon_\infty} - \frac{\delta_{ij}}{3\varepsilon_\infty} \right] . \tag{5.2}$$

The first term on the right-hand side of equation (5.2) gives the contribution only to longitudinal modes and is irrelevant to constructing the effective Hamiltonian. It is the second term that is the contribution of the dipole–dipole interaction to the transverse vibrational mode, and it leads to mode softening and its subsequent vanishing at the phase transition point. Actually, as shown in detail in Kvyatkovskiĭ's paper [56] (see also the review article in Ref. [16]), in crystals with polarizable ions the contribution of the dipole–dipole interaction to the optical vibrational modes is not described by formula (5.2); instead it has the form

$$\Phi_{ij}(q \to 0) = \frac{4\pi Z_{\mathrm{eff}}^2}{v_0} \left[\frac{\mathbf{q}_i \mathbf{q}_j}{q^2 \varepsilon_\infty} - \frac{\delta_{ij}}{\varepsilon_\infty + 2} \right] . \tag{5.3}$$

Thus, the effective Hamiltonian proposed by Zhong et al. [85] understates by a factor of $(\varepsilon_\infty + 2)/3\varepsilon_\infty$ the negative (in sign) contribution of the dipole–dipole interaction to the transverse optical vibrational mode. Such an understating is balanced to a certain extent in Ref. [85] by a corresponding lowering of the strength of the short-range repulsive forces, since they were calculated on the basis of the equality of the sums of the contributions of the short- and long-range forces to the value of the optical mode at $q \neq 0$, which, in turn, was calculated from first principles without any separation of contributions into short- and long-range interactions. The same procedure of adjusting the short-range repulsive forces led Zhong et al. [85] to an entirely erroneous conclusion that the ferroelectric transition point T_c depends only slightly on the value of the effective Born charge. The researchers found that as Z_{eff} changes by a factor of two the value of T_c changes by only 10%. Drawing this conclusion, the researchers did not account for the fact that in their procedure of separating the contributions they, by changing Z_{eff} by a factor of two, also changed the short-range repulsive forces. It comes as no surprise, therefore, that T_c changed very insignificantly. As a curiosity, we note that Rabe and Joannopoulos [84] calculated the thermodynamic properties of the ferroelectric compound GeTe without incorporating the dipole–dipole interaction into the effective Hamiltonian.

The work of our group, to which we now turn, amounted to studying the structural transitions caused by the instability of the vibrational modes at $q \neq 0$, where the problem of allowing for the dipole–dipole interaction can be solved much more simply than in the case where $q = 0$.

Here, we describe the use of the effective Hamiltonian method of calculating the transition temperatures and the thermodynamic properties of ionic crystals in combination with the formulas of Section 3 for calculating the total energy and the lattice vibration frequencies. As an example, we consider $Rb_2KB^{3+}F_6$ crystals (B^{3+} is Sc, In, and Lu) with the elpasolite structure, which undergo a structural transition from the cubic phase to the tetragonal [87–89]. The isomorphic crystals Rb_2KScF_6, Rb_2KInF_6, and Rb_2KLuF_6 in the high-temperature phase are characterized by the space group $Fm3m$ with ten atoms per unit cell (Fig. 7). As the temperature lowers, these crystals undergo a phase transition into the tetragonal phase with the space group $I4/m$ (the unit-cell volume does not change in the process). For these

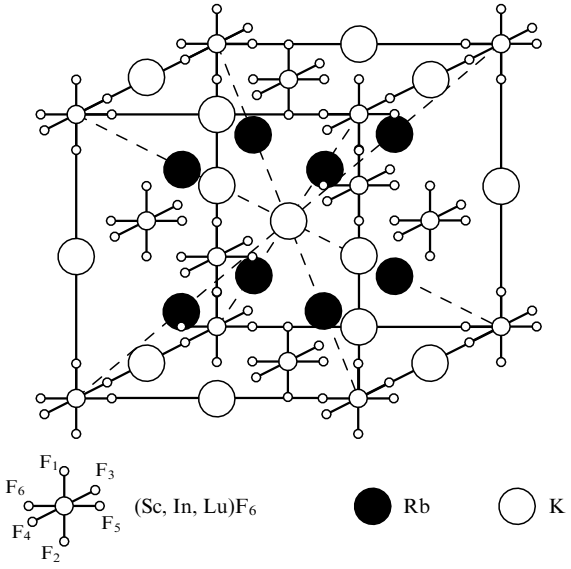

Figure 7. The structure of Rb_2KBF_6 crystals.

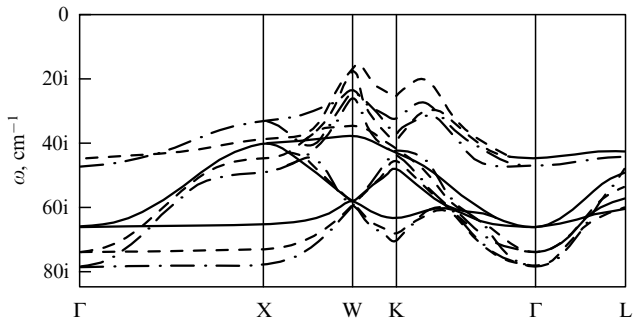

Figure 8. Calculated low-energy part of the spectrum $\omega(\mathbf{q})$ for Rb_2KBF_6 crystals. The solid curves correspond to $B = Sc$, the dashed curves correspond to $B = In$, and the dot-dash curves correspond to $B = Lu$.

crystals, the equilibrium volume, the dielectric constant, the Born dynamical charges, and the complete spectrum of lattice vibrations have been calculated in Refs [87–89]. Soft modes were detected in the vibrational spectrum of all three crystals, with the modes occupying the entire phase space. The low-energy and soft phonons for these crystals are shown in Fig. 8. Clearly, the most unstable modes are those belonging to the vibrational branch between $\Gamma\,(\mathbf{q} = 0, 0, 0)$ and $X\,(\mathbf{q} = 2\pi/a_0, 0, 0)$ points of the Brillouin zone. At Γ point the T_{1g} mode of this branch is threefold degenerate, while in the directions $\Gamma-X$, $\Gamma-Y$, and $\Gamma-Z$, including the boundary points, the low-lying modes are not degenerate. The threefold degenerate mode at $q = 0$ and the nondegenerate modes in the directions $\Gamma-X$, $\Gamma-Y$, and $\Gamma-Z$ correspond to vibrations in which the fluorine ions are displaced, with the displacements v_k^F in these modes related as follows:

$$
\begin{aligned}
& -v_{1y}^F = v_{2y}^F = v_{5z}^F = -v_{6z}^F\,,\\
T_{1g}: \quad & -v_{1x}^F = v_{2x}^F = -v_{3z}^F = v_{4z}^F\,,\\
& -v_{3y}^F = v_{4y}^F = -v_{5x}^F = v_{6x}^F\,,\\
X_3: \quad & -v_{1y}^F = v_{2y}^F = v_{5z}^F = -v_{6z}^F\,,\\
Y_3: \quad & -v_{1x}^F = v_{2x}^F = -v_{3z}^F = v_{4z}^F\,,\\
Z_3: \quad & -v_{3y}^F = v_{4y}^F = -v_{5x}^F = v_{6x}^F\,.
\end{aligned}
\tag{5.4}
$$

These displacements of the fluorine ions lead to a 'rotation' of the BF_6 octahedron.

To write the model Hamiltonian, we use the local mode approximation, in which the only degrees of freedom that are taken into account are those related to modes (5.4), assuming that the other degrees of freedom are inessential in the structural phase transition from the cubic phase to the tetragonal. Thus, for Rb_2KBF_6 crystal the local mode has the form

$$
S_\alpha = \frac{1}{a_0}\sum_k \xi_{\alpha k} v_k^F\,, \tag{5.5}
$$

where $\alpha = x, y, z$; v_k^F is the amplitude of the displacement of the kth fluorine atom taken from (5.4); the $\xi_{\alpha k}$ are the eigenvectors of the lattice vibrational mode (Table 5); and $a_0 = 16.26$ a.u. is the calculated lattice parameter for the cubic phase. Under symmetry operations of the highly symmetric cubic phase, the local mode (S_x, S_y, S_z) is transformed as a pseudovector.

It must be noted at this point that a local mode corresponding to a 'rotation' of the octahedron was used by Vanderbilt and Zhong [86] to build a model Hamiltonian that describes the structural phase transition in the $SrTiO_3$ crystal with the perovskite structure. However, in the perovskite structure, the SrO_6 octahedron is not a structural unit, each oxygen ion belongs to two neighboring octahedrons, and additional, somewhat artificial, assumptions have to be made in order to write an effective Hamiltonian with such a local mode [86]. There is no problem of this kind in the case of crystals with the elpasolite structure (which we are examining here), since in this structure the $B^{3+}F_6$ octahedron belongs to a single unit cell. What is also important is that the local mode (5.5) is not polar, i.e., no additional dipole moments appear in the vibrations, and there is no need to take into account the long-range dipole–dipole interactions when we set up the model Hamiltonian.

Thus, to describe the structural phase transition $Fm3m \to I4/m$, we set up the effective Hamiltonian according to the following procedure. The three-component local mode (a pseudovector) is placed in the sites of an fcc lattice. To simplify matters, into the effective Hamiltonian we incorporate the anharmonic terms for only a single-site potential. Here, we allow for all second- and fourth-order terms and a fraction of sixth-order anisotropic terms. The pair interactions between the local modes on different lattice sites are taken into account only within the first and second coordination spheres. Finally, the interaction between a local mode and the uniform (over the lattice) elastic strains is also taken into account.

We can now write the microscopic model Hamiltonian, where we have included the transformations of the local mode and the fcc lattice under cubic-symmetry operations:

$$
H = \sum_i (H_i^{\mathrm{anh}} + H_i^{SS}) + H^{Se} + H^{ee}\,,
$$

$$
H_i^{\mathrm{anh}} = B(S_{ix}^4 + S_{iy}^4 + S_{iz}^4) + C(S_{ix}^2 S_{iy}^2 + S_{iy}^2 S_{iz}^2 + S_{iz}^2 S_{ix}^2) + D(S_{ix}^6 + S_{iy}^6 + S_{iz}^6)\,,
$$

$$
H_i^{SS} = S_{ix}\left[AS_{ix} + a_1 \sum_{\mathbf{d}=(0,\pm1,\pm1)} S_x\left(\mathbf{R}_i + \frac{a_0\mathbf{d}}{2}\right) + a_2 \sum_{\mathbf{d}=\binom{\pm1,\pm1,0}{\pm1,0,\pm1}} S_x\left(\mathbf{R}_i + \frac{a_0\mathbf{d}}{2}\right)\right] + S_{ix}\left[a_3 \sum_{\mathbf{d}=(\pm1,0,\pm1)} (\mathbf{d}\cdot\mathbf{z})(\mathbf{d}\cdot\mathbf{x}) S_z\left(\mathbf{R}_i + \frac{a_0\mathbf{d}}{2}\right)\right.
$$

Table 5. Eigenvectors.

	Rb1	Rb2	F1	F2	F3	F4	F5	F6	K	B^{3+}
ξ_x	0 0 0	0 0 0	0 −0.5 0	0 0.5 0	0 0 0	0 0 0	0 0 0.5	0 0 −0.5	0 0 0	0 0 0
ξ_y	0 0 0	0 0 0	−0.5 0 0	0.5 0 0	0 0 −0.5	0 0 0.5	0 0 0	0 0 0	0 0 0	0 0 0
ξ_z	0 0 0	0 0 0	0 0 0	0 0 0	0 −0.5 0	0 0.5 0	−0.5 0 0	0.5 0 0	0 0 0	0 0 0

$$
\begin{aligned}
&+ a_3 \sum_{\mathbf{d}=(\pm1,\pm1,0)} (\mathbf{d}\cdot\mathbf{y})(\mathbf{d}\cdot\mathbf{x}) S_y\left(\mathbf{R}_i + \frac{a_0\mathbf{d}}{2}\right)\Bigg] \\
&+ S_{iy}\Bigg[AS_{iy} + a_1 \sum_{\mathbf{d}=(\pm1,0,\pm1)} S_y\left(\mathbf{R}_i + \frac{a_0\mathbf{d}}{2}\right) \\
&+ a_2 \sum_{\mathbf{d}=\begin{pmatrix}\pm1,\pm1,0\\0,\pm1,\pm1\end{pmatrix}} S_y\left(\mathbf{R}_i + \frac{a_0\mathbf{d}}{2}\right)\Bigg] \\
&+ S_{iy}\Bigg[a_3 \sum_{\mathbf{d}=(0,\pm1,\pm1)} (\mathbf{d}\cdot\mathbf{z})(\mathbf{d}\cdot\mathbf{y}) S_z\left(\mathbf{R}_i + \frac{a_0\mathbf{d}}{2}\right) \\
&+ a_3 \sum_{\mathbf{d}=(\pm1,\pm1,0)} (\mathbf{d}\cdot\mathbf{x})(\mathbf{d}\cdot\mathbf{y}) S_x\left(\mathbf{R}_i + \frac{a_0\mathbf{d}}{2}\right)\Bigg] \\
&+ S_{iz}\Bigg[AS_{iz} + a_1 \sum_{\mathbf{d}=(\pm1,\pm1,0)} S_z\left(\mathbf{R}_i + \frac{a_0\mathbf{d}}{2}\right) \\
&+ a_2 \sum_{\mathbf{d}=\begin{pmatrix}\pm1,0,\pm1\\0,\pm1,\pm1\end{pmatrix}} S_z\left(\mathbf{R}_i + \frac{a_0\mathbf{d}}{2}\right)\Bigg] \\
&+ S_{iz}\Bigg[a_3 \sum_{\mathbf{d}=(0,\pm1,\pm1)} (\mathbf{d}\cdot\mathbf{z})(\mathbf{d}\cdot\mathbf{y}) S_x\left(\mathbf{R}_i + \frac{a_0\mathbf{d}}{2}\right) \\
&+ a_3 \sum_{\mathbf{d}=(\pm1,0,\pm1)} (\mathbf{d}\cdot\mathbf{z})(\mathbf{d}\cdot\mathbf{x}) S_y\left(\mathbf{R}_i + \frac{a_0\mathbf{d}}{2}\right)\Bigg] \\
&\quad + S_{ix}\Bigg[b_1 \sum_{\mathbf{d}=(\pm1,0,0)} S_x(\mathbf{R}_i + a_0\mathbf{d}) \\
&\quad + b_2 \sum_{\mathbf{d}=\begin{pmatrix}0,\pm1,0\\0,0,\pm1\end{pmatrix}} S_x(\mathbf{R}_i + a_0\mathbf{d})\Bigg] \\
&\quad + S_{iy}\Bigg[b_1 \sum_{\mathbf{d}=(0,\pm1,0)} S_y(\mathbf{R}_i + a_0\mathbf{d}) \\
&\quad + b_2 \sum_{\mathbf{d}=\begin{pmatrix}\pm1,0,0\\0,0,\pm1\end{pmatrix}} S_y(\mathbf{R}_i + a_0\mathbf{d})\Bigg] \\
&\quad + S_{iz}\Bigg[b_1 \sum_{\mathbf{d}=(0,0,\pm1)} S_z(\mathbf{R}_i + a_0\mathbf{d}) \\
&\quad + b_2 \sum_{\mathbf{d}=\begin{pmatrix}\pm1,0,0\\0,0,\pm1\end{pmatrix}} S_z(\mathbf{R}_1 + a_0\mathbf{d})\Bigg], \qquad (5.6)
\end{aligned}
$$

$$
\begin{aligned}
H^{Se} &= g_1(e_1+e_2+e_3)\sum_i (S_{ix}^2 + S_{iy}^2 + S_{iz}^2) \\
&\quad + g_2\Bigg[(e_1+e_2-2e_3)\sum_i (S_{ix}^2 + S_{iy}^2 - 2S_{iz}^2) \\
&\quad + 3(e_1-e_2)\sum_i (S_{ix}^2 - S_{iy}^2)\Bigg] \\
&\quad + g_3\left(e_4\sum_i S_{iy}S_{iz} + e_5\sum_i S_{ix}S_{iz} + e_6\sum_i S_{ix}S_{iy}\right), \\
H^{ee} &= C_{11}(e_1+e_2+e_3) + C_{12}(e_1e_2 + e_2e_3 + e_3e_1) \\
&\quad + C_{44}(e_4^2 + e_5^2 + e_6^2).
\end{aligned}
$$

Here, $\mathbf{R}_i$ is the radius vector of the ith site of the crystal lattice; $\mathbf{x}$, $\mathbf{y}$, and $\mathbf{z}$ are the unit vectors directed along the axes of a Cartesian system of coordinates; and the C_{ij} are the elastic constants of the crystal lattice. The elastic strains e_i are given in Voigt's notation:

$$
\begin{aligned}
&e_1 = u_{11}, \quad e_2 = u_{22}, \quad e_3 = u_{33}, \\
&e_4 = 2u_{23}, \quad e_5 = 2u_{13}, \quad e_6 = 2u_{12}, \\
&u_{\alpha\beta} = \frac{1}{2}\left(\frac{\partial u_\alpha}{\partial x_\beta} + \frac{\partial u_\beta}{\partial x_\alpha}\right),
\end{aligned}
$$

where u_α is a displacement along the x_α axis.

The numerical values of the coefficients in the effective Hamiltonian (5.6) can be found by calculating the total energy and lattice dynamics of the crystal, as mentioned earlier in this section.

The coefficients of the second-order terms in (5.6) were determined on the basis of the calculated eigenvalues λ_i of the force-constants matrix with a vector $\mathbf{q}$ along the [100] direction and the total energies E_i of the distorted phases for the three crystals (Table 6).

The values of the elastic constants C_{11}, C_{12}, and C_{44} were found from the calculated dependences of the frequencies of the longitudinal and transverse acoustic vibrations at small q's for the three symmetric directions [001], [110], and [111]. Table 7 lists the calculated values of the elastic constants $C_{ij} = c_{ij}v_0$ of the Rb_2KBF_6 (B = Sc, In, and Lu). The coefficients B, C, and D of the anharmonic terms in the single-site potential were determined from the dependence of the total energy of a 'squeezed' crystal (i.e., with the lattice parameters of the cubic phase $a_0 = 16.26$, 16.72, and 16.67 a.u. for Rb_2KScF_6, Rb_2KInF_6, and Rb_2KLuF_6, respectively) on the angle of 'rotation' of the BF_6 octahedron about the [001] ($S_x = S_y = 0$ and $S_z = |S|$), [110] ($S_x = S_y = |S|$ and $S_z = 0$), and [111] ($S_x = S_y = S_z = |S|$) axes. Figure 9 shows, for instance, such a dependence of the energy on the 'rotation' of the octahedron about the [100] axis for the three crystals. The values of the coefficients B, C, and D adjusted by the least-squares method are listed in Table 7. Since no shear deformations appear in the tetragonal phase as a result of the phase transition $Fm3m \rightarrow I4/m$, the coefficient g_3 in (5.6) was not determined. The coefficients g_1 and g_2 were determined by the following technique. First the dependence

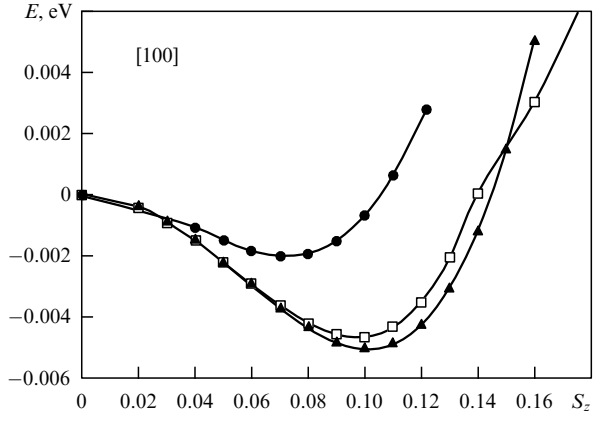

Figure 9. Total energy of Rb_2KBF_6 crystals in the tetragonal phase as a function of the angle of 'rotation' of the BF_6 octahedron about the [100] axis: ●, B = Sc; □, B = In; and ▲, B = Lu.

Table 6. The expressions for the distortion energies (in eV) $\Delta E_i = E_i - E_0 - E_{\text{anh}}$ of some phases; λ_i are the eigenvalues of the force matrix (in eV).

		Rb_2KScF_6	Rb_2KInF_6	Rb_2KLuF_6
ΔE_1; $\lambda_1(T_{1g})$	$4a_1 + 8a_2 + 2b_1 + 4b_2 + A$	−22.12	−26.91	−27.88
ΔE_X; $\lambda_2(X_2^+)$	$4a_1 - 8a_2 + 2b_1 + 4b_2 + A$	−21.68	−26.17	−28.04
$\mathbf{q} = \frac{\pi}{a_0}(1,0,0)$	$4a_1 - 2b_1 + 4b_2 + A$	−21.90	−21.17	−20.34
ΔE_1	$-24a_3 - 6b_1 - 12b_2 + 3A$	−6.50	18.41	10.45
ΔE_{zx}	$-4a_1 + 2b_1 + 4b_2 + A$	12.76	16.56	32.91

of the total energy of the 'free' crystal on the angle of the octahedron's 'rotation' about the [001] axis was determined, and for each value of the angle the energy was minimized in the unit-cell parameters and in the radii of the ions' Watson spheres. Then the total energy of the 'squeezed' crystal was subtracted from the above dependence, and the coefficients g_1 and g_2 were adjusted to this difference by the least-squares method with the already determined values of the elastic constants (the coefficients are listed in Table 7).

Despite its simplicity, the resulting effective Hamiltonian contains many parameters, and the calculation of the free energy and other thermodynamic quantities analytically by methods of the self-consistent field type is extremely difficult. Hence, the thermodynamic properties of a system with the effective Hamiltonian (5.6) are usually calculated by the numerical Monte Carlo technique [90]. The classical Metropolis Monte Carlo method [90] was used in Refs [88, 89] for an fcc lattice of the size $L \times L \times L$ with periodic boundary conditions. At each lattice site there was a three-component pseudovector S_x, S_y, S_z. The entire lattice is in the field of uniform strains e_1, e_2, and e_3. The Monte Carlo method was used to study two cases: a 'squeezed' crystal, i.e., without allowance for elastic strains ($e_1 = e_2 = e_3 = 0$), and a 'free' crystal, with e_1, e_2, and e_3 calculated in the Monte Carlo process. In the first case a single Monte Carlo step consisted in the following. Consecutively, an increment of the components of the pseudovector (S_{ix}, S_{iy}, S_{iz}) was chosen at random at each lattice site and the possibility of accepting this increment was verified. For each temperature, 50,000 Monte Carlo steps were made, and the averaging procedure needed for finding the thermodynamic properties was carried out in the last 10,000 steps in the standard way [90].

Table 7. Parameters of the effective Hamiltonian (in eV).

	Rb_2KScF_6	Rb_2KInF_6	Rb_2KLuF_6
	Single-site		
A	4.10	3.09	13.82
B	2.44×10^3	1.40×10^3	1.35×10^3
C	2.63×10^3	2.25×10^3	2.21×10^3
D	-40.70×10^3	-0.73×10^3	-1.16×10^3
	Interstitial		
a_1	−4.33	−5.39	−7.59
a_2	−0.03	−0.05	0.10
a_3	1.87	0.63	2.71
b_1	−0.00	−1.35	−1.90
b_2	−2.17	−1.35	−1.90
	Uniform-strain coupling coefficients		
g_1	118.5	39.88	53.00
g_2	−23.6	−15.92	−21.20
	Elastic constants		
C_{11}	50.0	53.6	68.6
C_{12}	12.8	11.7	18.7
C_{44}	18.2	9.5	3.4
	Transition temperature		
T^{calc}, K	250	550	660
T^{exp}, K	252	283	360

In the case of a 'free' crystal, after each Monte Carlo step described above an attempt was made to assign an increment to each component of the stress tensor. The increment was selected at random from the interval $[-0.03, 0.03]$. For each component, 1000 attempts were made, and then averaging was carried out. The resulting average values of the strain components and the configuration of the pseudovectors in each Monte Carlo step served as the initial data for the next step. The temperatures selected as the starting temperature were either high (1500 K) or low ($\approx$ 50 K). The Monte Carlo simulation starting at high temperatures was carried out from two initial configurations, with one configuration corresponding to the highly symmetric cubic phase ($S_{ix} = S_{iy} = S_{iz} = 0$) and the other to a distorted tetragonal phase ($S_{iz} = 0.08$ and $S_{ix} = S_{iy} = 0$). When the simulation was started at low temperatures, the initial configuration corresponded to the tetragonal phase. The calculations were done for the size $L = 10$ (4000 pseudovectors). Several temperatures were calculated for a large lattice with $L = 20$ (32,000 pseudovectors) for verification. The results of these calculations for the $20 \times 20 \times 20$ lattice almost perfectly coincided with the results of calculations for the $10 \times 10 \times 10$ lattice. The results of all these calculations led to values of the temperature of the phase transition from the cubic phase to the tetragonal and to the temperature dependence of the pseudovector components S_{ix}, S_{iy}, and S_{iz} and the components of the strain tensor e_1, e_2, and e_3. We have listed these results together with the well-known experimental data. Table 7 and Figs 10 and 11 show that the temperatures of the phase transitions from the cubic phase to the tetragonal and the temperature behavior of the order parameter and the components of the spontaneous strain tensor of the crystal in the distorted phase are in satisfactory agreement with the experimental data.

6. Conclusions

Let us now briefly formulate some conclusions that can be drawn from our discussion of the first-principles calculations of the physical properties of ionic crystals. First, we have shown that within the density functional theory there are at least two alternative approaches to such calculations. One of these, which is used most often, is based on a representation of the total electron density in a crystal as the density of a system

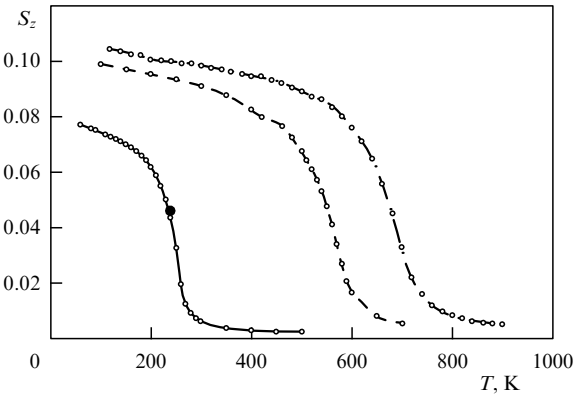

Figure 10. Temperature dependence of the order parameter in the tetragonal phase of Rb_2KBF_6 crystals: the solid curve corresponds to B = Sc, the dashed curve corresponds to B = In, and the dot-dash curve corresponds to B = Lu. The full circle indicates the experimental value of S_z extracted from the experimental data on the structure of Rb_2KScF_6 at T = 240 K [Flerov I N et al. *Material Sci. Engin.* **R24** 81 (1998)].

of noninteracting electrons that are in a self-consistent potential of some sort. The electrons in this approach are described by Bloch wave functions that are used for calculating the dielectric properties of crystals.

The second approach, developed mainly by the present authors, is based on a representation of the total electron density as a superposition of the densities of the individual ions. The approach does not use, even theoretically, the concept of a total electron wave function, and all calculations of the properties of a crystal use only the electron density.

Naturally, both approaches have their advantages and disadvantages. The main advantage of the first approach is its universality. It can be used in calculations for ionic crystals, for metals, and for covalent semiconductors. Beginning with the 1930s, powerful computational methods were developed to solve the main problem in this approach, the wave equation for electrons in a periodic potential. These methods made it possible to solve with high accuracy the Kohn–Sham wave equation proper and to carry out calculations of all the ground state properties of a crystal. What is more, this approach provided the well-known expression for the exchange-correlation energy as a density functional, at least in the local approximation. At present there exists a whole spectrum of quite reasonable suggestions on how to go beyond the local approximation.

But this approach also has disadvantages. One of these is the need to carry out cumbersome and time-consuming calculations and, as a rule, to use powerful supercomputers. Of course, in view of the rapid progress in computer techniques, the role of this drawback in the use of the Kohn–Sham method is constantly diminishing. We believe that there is one more drawback in this approach, a drawback that manifests itself most vividly in the study of ionic crystals. The thing is that the universality of this approach, i.e., the use of the Bloch representation for the wave functions of electrons in crystals of any type, in some cases leads to a loss in physical clarity in understanding the nature of the phenomena that take place in specific crystals. A vivid example of this is the fact that the very definition of electron polarization within the Kohn–Sham method was formulated only recently via an elegant, but fairly abstract, method, the Berry phase method. This led, as the present review shows, to a situation in which some researchers simply ignored all the physics of ionic crystals that existed before the Berry phase method was developed; this is true, in particular, of the relation between the electric polarization of the crystal and the appearance of a dipole moment in each unit cell. The present review also mentions a number of other inaccurate conclusions and statements made by some researchers in the study of ionic crystals using the Kohn–Sham method.

In this respect, the second approach covered in this review has an indubitable advantage. As shown in the present review, the approach may be considered to a large extent as a microscopic justification of the old (but not necessarily wrong) phenomenological models of a deformable and polarizable ion. Moreover, it retains the simplicity and clarity of the previous theories of ionic crystals. Within this approach, as in the 'old' phenomenological theories, one

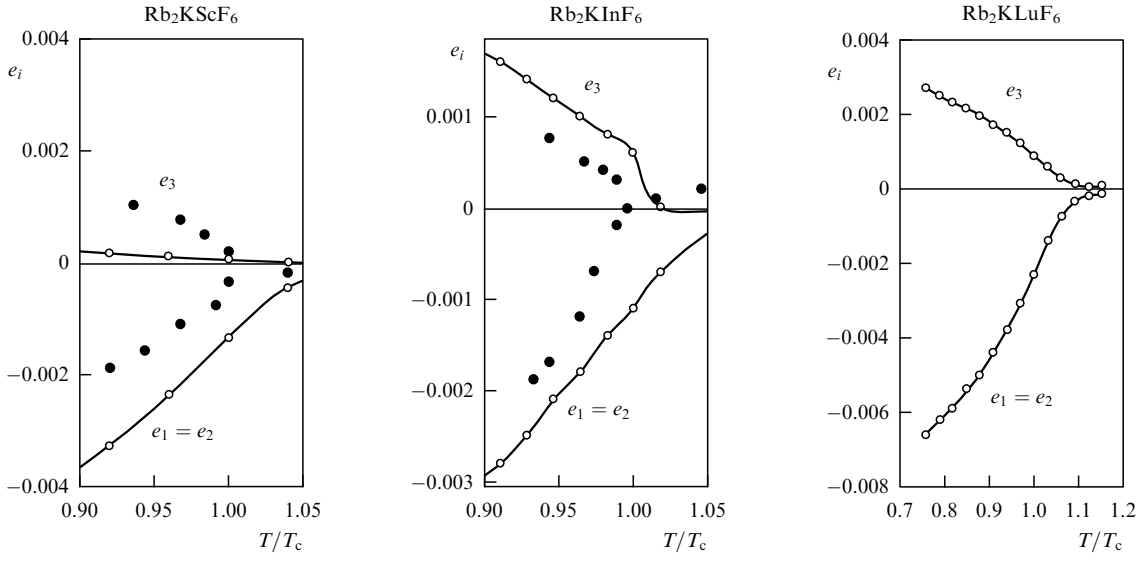

Figure 11. Temperature dependence of the components of the strain tensor in the tetragonal phase. Open circles correspond to the Monte Carlo data and full circles correspond to the experimental data (Flerov I N et al. *Fiz. Tverd. Tela* **34** 2185, 3493 (1992) [*Sov. Phys. Solid State* **34** 1168, 1870 (1992)]).

can clearly see the role that non-Lorentz local-field corrections play in the phenomenon of electric polarization in perovskite crystals. It also clarifies the problem of ferroelectric instability caused by dipole–dipole interactions between unit cells in the optically active mode. Moreover, our calculations have clearly shown that quadrupole distortion of the oxygen electron density plays a distinctive role in the phenomenon of ferroelectric instability: such distortion facilitates stabilization of a soft optical mode, since in the absence of a quadrupole moment on the oxygen atom many perovskite crystals would be pyroelectrics rather than ferroelectrics.

Of course, as in every method, there are disadvantages to our approach, and some of these stem from the advantages. For instance, all multipole distortions of the ion electron density were calculated in first-order perturbation theory in the external potential. This technique simplifies and speeds up calculations substantially. Our results and a comparison of the electron density distributions in ionic crystals that we calculated with the experimental data and with the results of calculations using the Kohn–Sham method show that the change in the electron density on an ion does indeed vary only slightly when the ion is placed inside a crystal. Such an assumption may prove incorrect in the case of metals or covalent semiconductors.

Another approximation of our approach is the use of the Thomas–Fermi functional in describing the electron energy of a crystal. On the one hand, this simplifies and speeds-up all calculations even more. On the other hand, we end up with an incorrect description of the ion–ion interaction over large distances. In our original papers we developed a number of tools to neutralize this drawback. In particular, in calculations of the total energy we used the Ewald method to evaluate the contribution of long-range interactions between point Coulomb objects, contributions that are specified automatically in the given approach. To allow for short-range forces caused by the overlap of the ion electron densities, we reduced the problem of calculating the crystal's energy to that of calculating the energy of a single unit cell. The tails of the electron densities of all the ions were projected into this cell. In this way we allowed for the contribution of all many-body interactions caused by the overlap of all electron shells rather than the shells of two ions. Furthermore, bearing in mind that ionic crystals, as a rule, have close-packed structures, such a procedure widens the limits of applicability of the Thomas–Fermi functional because of the increase in the electron density in a single unit cell.

In conclusion, we would like to express our deep gratitude to our many colleagues and friends for the fruitful discussions and their help in our research. Special thanks go to V L Ginzburg for his constant support of our efforts in studying ionic crystals. We are grateful to O E Kvyatkovskiĭ for our fruitful cooperation over the years, and to O V Ivanov, who contributed greatly to the development of the computer realization of the microscopic first-principles method of a polarizable and deformable ion, which was described in this article. This work was made possible by the financial support from the Russian Foundation for Basic Research (Grants Nos 02-02-16658 and 03-02-16076), the Presidential Program Supporting Scientific Schools and Scientific Programs of the Russian Academy of Sciences, and the NWO–RFBR Grant No. 0.47.016.005.

References

1. Jensen H, Lenz W *Z. Phys.* **77** 722 (1932)
2. Thomas L H *Proc. Cambr. Philos. Soc.* **23** 542 (1926)
3. Fermi E *Z. Phys.* **48** 73 (1928)
4. Lundqvist S, March N H (Eds) *Theory of the Inhomogeneous Electron Gas* (New York: Plenum Press, 1983) [Translated into Russian (Moscow: Mir Publ., 1986)]
5. Kirzhnits D A *Polevye Metody Teorii Mnogikh Chastits* (Field Theoretical Methods in Many-Body Systems) (Moscow: Atomizdat, 1963) [Translated into English (Oxford: Pergamon Press, 1967)]
6. Kirzhnits D A, Lozovik Yu E, Shpatakovskaya G V *Usp. Fiz. Nauk* **117** 3 (1975) [*Sov. Phys. Usp.* **18** 649 (1976)]
7. Ashcroft N W, Mermin N D *Solid State Physics* (New York: Holt, Rinehart and Winston, 1976) [Translated into Russian (Moscow: Mir, 1979)]
8. Slater J C *Quantum Theory of Molecules and Solids* Vol. 3 *Insulators, Semiconductors, and Metals* (New York: McGraw-Hill, 1967) [Translated into Russian (Moscow: Mir, 1969)
9. Born M, Huang K *Dynamical Theory of Crystal Lattices* (New York: Clarendon Press, 1954) [Translated into Russian (Moscow: IL, 1958)]
10. Kunc K, Balkanski M, Nusimovici M A *Phys. Rev. B* **12** 4346 (1975)
11. Löwdin P D *Ark. Mat. Astr. Fys.* (Sweden) **35a** 30 (1947)
12. Tolpygo K B *Zh. Eksp. Teor. Fiz.* **20** 497 (1950)
13. Abarenkov I V, Antonova I M *Phys. Status Solidi* **38** 783 (1970)
14. Zeyher R *Phys. Rev. Lett.* **35** 174 (1975)
15. Sinha S K, Gupta R P, Price D L *Phys. Rev. B* **9** 2564 (1974)
16. Kvyatkovskiĭ O E, Maksimov E G *Usp. Fiz. Nauk* **154** 3 (1988) [*Sov. Phys. Usp.* **31** 1 (1988)]
17. Hohenberg P, Kohn W *Phys. Rev.* **136** B864 (1964)
18. Kohn W, Sham L J *Phys. Rev.* **140** A1133 (1965)
19. Kohn W *Rev. Mod. Phys.* **71** 1253 (1999); *Usp. Fiz. Nauk* **172** 336 (2002)
20. Perdew J P, Kurth S, in *Density Functional: Theory and Applications* (Lecture Notes in Physics, Vol. 500, Ed. D Joubert) (Berlin: Springer, 1998) p. 8
21. Mattheiss L F *Phys. Rev. B* **6** 4718 (1972)
22. Cohen R E, Krakauer H *Ferroelectrics* **136** 65 (1992)
23. King-Smith R D, Vanderbilt D *Phys. Rev. B* **49** 5828 (1994)
24. Resta R *Rev. Mod. Phys.* **66** 899 (1994)
25. Resta R *J. Phys.: Condens. Matter* **14** R625 (2002)
26. Landau L D, Lifshitz E M *Elektrodinamika Sploshnykh Sred* (Electrodynamics of Continuous Media) 2nd ed. (Moscow: Nauka, 1982) p. 56 [Translated into English (Oxford: Pergamon Press, 1984)]
27. Martin R M *Phys. Rev. B* **9** 1998 (1974)
28. Tagantsev A K *Usp. Fiz. Nauk* **152** 423 (1987) [*Sov. Phys. Usp.* **30** 588 (1987)]
29. Tagantsev A K *Phase Transit.* **35** 119 (1991)
30. Kvyatkovskiĭ O E *Fiz. Tverd. Tela* **38** 101 (1996) [*Phys. Solid State* **38** 54 (1996)]
31. Kvyatkovskiĭ O E *Fiz. Tverd. Tela* **38** 728 (1996) [*Phys. Solid State* **38** 402 (1996)]
32. Bennett B I, Maradudin A A *Phys. Rev. B* **5** 4146 (1972)
33. Blount E I, in *Solid State Physics* Vol. 13 (Eds H Ehrenreich, F Seitz, D Turnbull) (New York: Academic Press, 1962) p. 305
34. Resta R *Ferroelectrics* **136** 51 (1992)
35. King-Smith R D, Vanderbilt D *Phys. Rev. B* **47** 1651 (1993)
36. Thouless D J et al. *Phys. Rev. Lett.* **49** 405 (1982)
37. Berry M V *Proc. R. Soc. London. Ser. A* **392** 45 (1984)
38. Kvyatkovskii O E *J. Korean Phys. Soc.* **32** 5140 (1998)
39. Kim Y S, Gordon R G *Phys. Rev. B* **9** 3548 (1974)
40. Kellermann E M *Philos. Trans. R. Soc. London Ser. A* **238** 513 (1940)
41. Yoder D R, Colella R *Phys. Rev. B* **25** 2545 (1982)
42. Boyer L L et al. *Phys. Rev. Lett.* **54** 1940 (1985)
43. Muhlhausen C, Gordon R G *Phys. Rev. B* **23** 900 (1981)
44. Wolf G H, Bukowinski M S *Phys. Chem. Miner.* **15** 69 (1988)
45. Watson R E *Phys. Rev.* **111** 1108 (1958)
46. Mahan G D, Subbaswamy K R *Local Density Theory of Polarizability* (New York: Plenum Press, 1990)
47. Leontovich M A *Vvedenie v Termodinamiku* (Introduction to Thermodynamics) 2nd ed. (Moscow: Nauka, 1983)

48. Ivanov O V, Maksimov E G *Solid State Commun.* **81** 69 (1992)
49. Ivanov O V, Maksimov E G *Phys. Rev. Lett.* **69** 108 (1992)
50. Ivanov O V, Maksimov E G *Zh. Eksp. Teor. Fiz.* **108** 1841 (1995) [*JETP* **81** 1008 (1995)]
51. Ivanov O V, Maksimov E G *Solid State Commun.* **97** 163 (1996)
52. Maksimov E G, Shport D A, Ivanov O V *Solid State Commun.* **101** 393 (1997)
53. Ivanov O V, Shport D A, Maksimov E G *Zh. Eksp. Teor. Fiz.* **114** 333 (1998) [*JETP* **87** 186 (1998)]
54. Zamkova N G, Zinenko V I *Fiz. Tverd. Tela* **40** 350 (1998) [*Phys. Solid State* **40** 320 (1998)]
55. Sternheimer R M *Phys. Rev.* **96** 951 (1954)
56. Kvyatkovskiĭ O E *Fiz. Tverd. Tela* **35** 2154 (1993) [*Phys. Solid State* **35** 1071 (1993)]
57. Mahan G D *Phys. Rev.* **153** 983 (1967)
58. Falter C et al. *Phys. Rev. B* **60** 12051 (1999)
59. Falter C, Hoffmann G A *Phys. Rev. B* **61** 14537 (2000)
60. Chizmeshya A et al. *Phys. Rev. B* **50** 15559 (1994)
61. Mehl M J, Hemley R J, Boyer L L *Phys. Rev. B* **33** 8685 (1986)
62. Zamkova N G et al. *Ferroelectrics* **283** 49 (2003)
63. Zhong W, King-Smith R D, Vanderbilt D *Phys. Rev. Lett.* **72** 3618 (1994)
64. Ghosez Ph et al. *Phys. Rev. B* **60** 836 (1999)
65. Fu L et al. *Phys. Rev. B* **57** 6967 (1998)
66. Yu R, Wang C Z, Krakauer H *Ferroelectrics* **164** 161 (1995)
67. Postnikov A V, Neumann T, Borstel G *Ferroelectrics* **164** 101 (1995)
68. Waghmare U V, Rabe K M *Phys. Rev. B* **55** 6161 (1997)
69. Lasota C et al. *Ferroelectrics* **194** 109 (1997)
70. Ghosez Ph, Gonze X, Mishenaud J-P *Ferroelectrics* **206–207** 285 (1998)
71. Ivanov O V, Maksimov E G, Mazin I I *Solid State Commun.* **76** 1267 (1990)
72. Flocken J W et al. *Phys. Rev. B* **31** 7252 (1985)
73. Boyer L L, Hardy J R *Phys. Rev. B* **24** 2577 (1981)
74. Zinenko V I, Zamkova N G *Fiz. Tverd. Tela* **42** 1310 (2000) [*Phys. Solid State* **42** 1348 (2000)]
75. Aleksandrov K S et al. *Zh. Eksp. Teor. Fiz.* **121** 1139 (2002) [*JETP* **94** 977 (2002)]
76. Wilson M, Schönberger U, Finnis M W *Phys. Rev. B* **54** 9147 (1996)
77. Wilson M, Madden P A *J. Phys.: Condens. Matter* **6** 159 (1994)
78. Cohen R E, Mehl M J, Boyer L L *Physica B+C* **150** 1 (1988)
79. Zinenko V I, Zamkova N G, Sofronova S N *Zh. Eksp. Teor. Fiz.* **123** 846 (2003) [*JETP* **96** 747 (2003)]
80. Longo J M, Kafalas J A *J. Solid State Chem.* **3** 429 (1971)
81. Gong Z, Cohen R E *Ferroelectrics* **136** 113 (1992)
82. Edwardson P J, Hardy J R *Phys. Rev. B* **38** 2250 (1988)
83. Rabe K M, Waghmare U V *Ferroelectrics* **164** 15 (1996)
84. Rabe K M, Joannopoulos J D *Phys. Rev. B* **36** 6631 (1987)
85. Zhong W, Vanderbilt D, Rabe K M *Phys. Rev. B* **52** 6301 (1995)
86. Vanderbilt D, Zhong W *Ferroelectrics* **206** 181 (1998)
87. Zinenko V I, Zamkova N G, Sofronova S N *Zh. Eksp. Teor. Fiz.* **114** 1742 (1998) [*JETP* **87** 944 (1998)]
88. Zinenko V I, Zamkova N G *Zh. Eksp. Teor. Fiz.* **118** 359 (2000) [*JETP* **91** 314 (2000)]
89. Zinenko V I, Zamkova N G *Fiz. Tverd. Tela* **43** 2193 (2001) [*Phys. Solid State* **43** 2290 (2001)]
90. Binder K (Ed.) *Monte Carlo Methods in Statistical Physics* (Berlin: Springer, 1979) [Translated into Russian (Moscow: Mir, 1982)]